

Predictive Heterogeneity: Measures and Applications

Jiashuo Liu*

*Department of Computer Science and Technology
Tsinghua University*

LIUJIASHUO77@GMAIL.COM

Jiayun Wu*

*Department of Computer Science and Technology
Tsinghua University*

JIAYUN.WU.WORK@GMAIL.COM

Bo Li

*School of Economics and Management
Tsinghua University*

LIBO@SEM.TSINGHUA.EDU.CN

Peng Cui†

*Department of Computer Science and Technology
Tsinghua University*

CUIP@TSINGHUA.EDU.CN

Abstract

As an intrinsic and fundamental property of big data, data heterogeneity exists in a variety of real-world applications, such as precision medicine, autonomous driving, financial applications, etc. For machine learning algorithms, the ignorance of data heterogeneity will greatly hurt the generalization performance and the algorithmic fairness, since the prediction mechanisms among different sub-populations are likely to differ from each other. In this work, we focus on the data heterogeneity that affects the prediction of machine learning models, and firstly propose the *usable predictive heterogeneity*, which takes into account the model capacity and computational constraints. We prove that it can be reliably estimated from finite data with probably approximately correct (PAC) bounds. Additionally, we design a bi-level optimization algorithm to explore the usable predictive heterogeneity from data. Empirically, the explored heterogeneity provides insights for sub-population divisions in income prediction, crop yield prediction and image classification tasks, and leveraging such heterogeneity benefits the out-of-distribution generalization performance.

Keywords: Predictive Heterogeneity, Out-of-Distribution Generalization, Computation Constraints

1 Introduction

Big Data provides great opportunities for the growth and advancement of Artificial Intelligence (AI) systems. Nowadays, AI has emerged as a ubiquitous tool that permeates almost every aspect of the contemporary technological landscape, making it an indispensable asset in various fields and industries, such as scientific discoveries, policy-making, healthcare, drug discovery, and so on. However, along with the widespread deployment of AI systems, the reliability, fairness, and stability of AI algorithms have been increasingly doubted. For example, in sociological research (Tipton et al., 2020), studies have shown that even for carefully designed randomized trials, there are huge selection biases, making

*. Equal Contributions.

†. Corresponding Author.

scientific discoveries unreliable; in disease diagnosis, studies (Wynants et al., 2020; Roberts et al., 2021) have found hundreds of existing AI algorithms fail to detect and prognosticate for COVID-19 using chest radiographs and CT scans; in social welfare, decision support AI systems for credit loan applications are found to exhibit biases against certain demographic groups (Hardt et al., 2016; Verma, 2019); in various machine learning tasks, algorithms are faced with severely poor generalization performances under distributional shifts (Shen et al., 2021), etc. Another well-known example is Simpson’s paradox, which brings false discoveries to the social research (Wagner, 1982; Hernán et al., 2011).

In order to mitigate the barriers that inhibit the deployment of AI systems in crucial, high-stakes applications, numerous researchers have taken recourse to the established research paradigm of model-centric AI, whereby they endeavor to develop innovative algorithms aimed at addressing these challenges. However, in contemporary discourse about machine learning, it is increasingly evident that the challenges faced by algorithms extend beyond their intrinsic properties and extend to the nature of the data utilized in training these models. Specifically, the heterogeneity of data employed has emerged as a pivotal factor underlying these issues. The concept of data heterogeneity encompasses the *diversity* that exists within data, including *variations in data sources, generation mechanisms, sub-populations, and data structures*. Failure to account for such diversity in AI systems can lead to overemphasis on patterns found only in dominant sub-populations or groups, thereby resulting in false scientific discoveries, unreliable and inequitable decision-making, and poor generalization performance when confronted with new data. Given the high-stakes scenarios in which trustworthy AI is required, addressing the problem of data heterogeneity - an inherent property of big data - should receive increased attention. Moreover, in the current era of big models, where model development is approaching its limits, *researchers have huge opportunities to explore the intricacies of big data*, thereby facilitating the development of AI in parallel with the advancement of AI models and algorithms.

Despite its widespread existence, due to its complexity, data heterogeneity has not converged to a uniform formulation so far, and has different meanings among different fields. Li and Reynolds (1995) define the heterogeneity in *ecology* based on the system property and complexity or variability. Rosenbaum (2005) views the uncertainty of the potential outcome as unit heterogeneity in observational studies in *economics*. More recently, in machine learning, several works of *causal learning* (Peters et al., 2016; Arjovsky et al., 2019; Koyama and Yamaguchi, 2020; Liu et al., 2021a; Creager et al., 2021) and *robust learning* (Sagawa et al., 2019; Liu et al., 2022) leverage heterogeneous data from multiple environments to improve the out-of-distribution generalization ability. However, previous works have not provided a precise definition or sound quantification. In this work, targeting at the prediction task in machine learning, from the perspective of *prediction power*, we propose the predictive heterogeneity, a *new type* of data heterogeneity.

From a machine learning perspective, a major concern is the potential adverse effects of data heterogeneity on prediction accuracy. In this study, we propose predictive heterogeneity, which refers to the heterogeneity of data that impacts the performance of machine learning models. Our goal is to facilitate the development of machine learning systems by addressing this issue. To this end, we introduce a precise definition of predictive heterogeneity that quantifies the maximal additional predictive information that can be obtained by dividing the entire data distribution into sub-populations. This measure takes into account

the model capacity and computational constraints and can be accurately estimated from finite samples with probably approximately correct (PAC) bounds. We conduct a theoretical analysis of the properties of this measure and examine it under typical scenarios of data heterogeneity. In addition, we propose the information maximization (IM) algorithm to empirically explore the predictive heterogeneity within data. Through our empirical investigations, we find that the explored heterogeneity is interpretable and provides valuable insights for sub-population divisions in various fields, such as agriculture, sociology, object recognition, and healthcare. Moreover, the identified sub-populations can be utilized to identify features related to Covid-19 mortality and enhance the out-of-distribution generalization performance of machine learning models. This has been confirmed through experiments with both simulated and real-world data. In conclusion, our study contributes to the development of machine learning systems by providing a precise definition of predictive heterogeneity and a reliable measure for its estimation. Our findings demonstrate the potential of the IM algorithm for exploring predictive heterogeneity, assisting scientific discoveries and improving the generalization performance of machine learning models in real-world applications.

2 Preliminaries on Mutual Information and Predictive \mathcal{V} -Information

In this section, we briefly introduce the mutual information and predictive \mathcal{V} -information (Xu et al., 2020) which are the preliminaries of our proposed predictive heterogeneity.

Notations. For a probability triple $(\mathbb{S}, \mathcal{F}, \mathbb{P})$, define random variables $X : \mathbb{S} \rightarrow \mathcal{X}$ and $Y : \mathbb{S} \rightarrow \mathcal{Y}$ where \mathcal{X} is the covariate space and \mathcal{Y} is the target space. Accordingly, $x \in \mathcal{X}$ denotes the covariates, and $y \in \mathcal{Y}$ denotes the target. Denote the set of random categorical variables as $\mathcal{C} = \{C : \mathbb{S} \rightarrow \mathbb{N} | \text{supp}(C) \text{ is finite}\}$. Additionally, $\mathcal{P}(\mathcal{X}), \mathcal{P}(\mathcal{Y})$ denote the set of all probability measures over the Borel algebra on the spaces \mathcal{X}, \mathcal{Y} respectively. $H(\cdot)$ denotes the Shannon entropy of a discrete random variable and the differential entropy of a continuous variable, and $H(\cdot|\cdot)$ denotes the conditional entropy of two random variables.

In information theory, the mutual information of two random variables X, Y measures the dependence between the two variables, which quantifies the reduction of entropy for one variable when observing the other:

$$\mathbb{I}(X; Y) = H(Y) - H(Y|X). \quad (1)$$

It is known that the mutual information is associated with the predictability of Y (Cover Thomas and Thomas Joy, 1991). While the standard definition of mutual information unrealistically assumes the unbounded computational capacity of the predictor, rendering it hard to estimate especially in high dimensions. To mitigate this problem, Xu et al. (2020) raise the predictive \mathcal{V} -information under realistic computational constraints, where the predictor is only allowed to use models in the predictive family \mathcal{V} to predict the target variable Y .

Definition 1 (Predictive Family (Xu et al., 2020)) Let $\Omega = \{f : \mathcal{X} \cup \{\emptyset\} \rightarrow \mathcal{P}(\mathcal{Y})\}$. We say that $\mathcal{V} \subseteq \Omega$ is a predictive family if it satisfies:

$$\forall f \in \mathcal{V}, \quad \forall P \in \text{range}(f), \quad \exists f' \in \mathcal{V}, \quad \text{s.t. } \forall x \in \mathcal{X}, f'[x] = P, f'[\emptyset] = P. \quad (2)$$

A predictive family contains all predictive models that are allowed to use, which forms computational or statistical constraints. The additional condition in Equation 2 means that the predictor can always ignore the input covariates (x) if it chooses to (only use \emptyset).

Definition 2 (Predictive \mathcal{V} -information (Xu et al., 2020)) *Let X, Y be two random variables taking values in $\mathcal{X} \times \mathcal{Y}$ and \mathcal{V} be a predictive family. The predictive \mathcal{V} -information from X to Y is defined as:*

$$\mathbb{I}_{\mathcal{V}}(X \rightarrow Y) = H_{\mathcal{V}}(Y|\emptyset) - H_{\mathcal{V}}(Y|X), \quad (3)$$

where $H_{\mathcal{V}}(Y|\emptyset)$, $H_{\mathcal{V}}(Y|X)$ are the predictive conditional \mathcal{V} -entropy defined as:

$$H_{\mathcal{V}}(Y|X) = \inf_{f \in \mathcal{V}} \mathbb{E}_{x, y \sim X, Y}[-\log f[x](y)]. \quad (4)$$

$$H_{\mathcal{V}}(Y|\emptyset) = \inf_{f \in \mathcal{V}} \mathbb{E}_{y \sim Y}[-\log f[\emptyset](y)]. \quad (5)$$

Notably that $f \in \mathcal{V}$ is a mapping: $\mathcal{X} \cup \{\emptyset\} \rightarrow \mathcal{P}(\mathcal{Y})$, so $f[x] \in \mathcal{P}(\mathcal{Y})$ is a probability measure on \mathcal{Y} , and $f[x](y) \in \mathbb{R}$ is the density evaluated on $y \in \mathcal{Y}$. $H_{\mathcal{V}}(Y|\emptyset)$ is also denoted as $H_{\mathcal{V}}(Y)$.

Compared with the mutual information, the predictive \mathcal{V} -information restricts the computational power and is much easier to estimate in high-dimensional cases. When the predictive family \mathcal{V} contains all possible models, i.e. $\mathcal{V} = \Omega$, it is proved that $\mathbb{I}_{\mathcal{V}}(X \rightarrow Y) = \mathbb{I}(X; Y)$ (Xu et al., 2020).

3 Predictive Heterogeneity

In this paper, from the machine learning perspective, we quantify the data heterogeneity that affects decision making, named Predictive Heterogeneity, which is easy to integrate with machine learning algorithms and could help analyze big data and build more rational algorithms.

3.1 Interaction Heterogeneity

To formally define the predictive heterogeneity, we begin with the formulation of the interaction heterogeneity. The *interaction heterogeneity* is defined as:

Definition 3 (Interaction Heterogeneity) *Let X, Y be random variables taking values in $\mathcal{X} \times \mathcal{Y}$. Denote the set of random categorical variables as \mathcal{C} , and take its subset $\mathcal{E} \subseteq \mathcal{C}$. Then \mathcal{E} is an environment set iff there exists $\mathcal{E} \in \mathcal{E}$ such that $X, Y \perp\!\!\!\perp \mathcal{E}$. $\mathcal{E} \in \mathcal{E}$ is called an environment variable. The interaction heterogeneity between X and Y w.r.t. the environment set \mathcal{E} is defined as:*

$$\mathcal{H}^{\mathcal{E}}(X, Y) = \sup_{\mathcal{E} \in \mathcal{E}} \mathbb{I}(Y; X|\mathcal{E}) - \mathbb{I}(Y; X). \quad (6)$$

Each environment variable \mathcal{E} represents a stochastic ‘partition’ of $\mathcal{X} \times \mathcal{Y}$, and the condition for the environment set implies that there exists such a stochastic partition that the joint distribution of X, Y could be preserved in each environment. In information theory, $\mathbb{I}(Y; X|\mathcal{E}) - \mathbb{I}(Y; X)$ is called the *interaction information*, which measures the influence of the environment variable \mathcal{E} on the amount of information shared between the target Y and

the covariate X . And the *interaction heterogeneity* defined in Equation 6 quantifies the *maximal* additional information that can be gained from involving or uncovering the environment variable \mathcal{E} . Intuitively, large $\mathcal{H}^{\mathcal{E}}(X, Y)$ indicates that the predictive power from X to Y is enhanced by \mathcal{E} , which means that uncovering the latent sub-population associated with the environment partition \mathcal{E} will benefit the $X \rightarrow Y$ prediction.

3.2 Predictive Heterogeneity

Based on the mutual information, the computation of the interaction heterogeneity is quite hard, since the standard mutual information is notoriously difficult to estimate especially in big data scenarios. Also, even if the mutual information could be accurately estimated, the prediction model may not be able to make good use of it.

Inspired by Xu et al. (2020), we raise the *Predictive Heterogeneity*, which measures the interaction heterogeneity that can be captured under computational constraints and affects the prediction of models within the specified predictive family. To begin with, we propose the *Conditional Predictive \mathcal{V} -information*, which generalizes the predictive \mathcal{V} -information.

Definition 4 (Conditional Predictive \mathcal{V} -information) *Let X, Y be two random variables taking values in $\mathcal{X} \times \mathcal{Y}$ and \mathcal{E} be an environment variable. For a predictive family \mathcal{V} , the conditional predictive \mathcal{V} -information is defined as:*

$$\mathbb{I}_{\mathcal{V}}(X \rightarrow Y|\mathcal{E}) = H_{\mathcal{V}}(Y|\emptyset, \mathcal{E}) - H_{\mathcal{V}}(Y|X, \mathcal{E}), \quad (7)$$

where $H_{\mathcal{V}}(Y|\emptyset, \mathcal{E})$ and $H_{\mathcal{V}}(Y|X, \mathcal{E})$ are defined as:

$$H_{\mathcal{V}}(Y|X, \mathcal{E}) = \mathbb{E}_{e \sim \mathcal{E}} \left[\inf_{f \in \mathcal{V}} \mathbb{E}_{x, y \sim X, Y|\mathcal{E}=e} [-\log f[x](y)] \right]. \quad (8)$$

$$H_{\mathcal{V}}(Y|\emptyset, \mathcal{E}) = \mathbb{E}_{e \sim \mathcal{E}} \left[\inf_{f \in \mathcal{V}} \mathbb{E}_{y \sim Y|\mathcal{E}=e} [-\log f[\emptyset](y)] \right]. \quad (9)$$

Intuitively, the conditional predictive \mathcal{V} -information measures the weighted average of predictive \mathcal{V} -information among environments. And here we are ready to formalize the predictive heterogeneity measure.

Definition 5 (Predictive Heterogeneity) *Let X, Y be random variables taking values in $\mathcal{X} \times \mathcal{Y}$ and \mathcal{E} be an environment set. For a predictive family \mathcal{V} , the predictive heterogeneity for the prediction $X \rightarrow Y$ with respect to \mathcal{E} is defined as:*

$$\mathcal{H}_{\mathcal{V}}^{\mathcal{E}}(X \rightarrow Y) = \sup_{\mathcal{E} \in \mathcal{E}} \mathbb{I}_{\mathcal{V}}(X \rightarrow Y|\mathcal{E}) - \mathbb{I}_{\mathcal{V}}(X \rightarrow Y), \quad (10)$$

where $\mathbb{I}_{\mathcal{V}}(X \rightarrow Y)$ is the predictive \mathcal{V} -information following from Definition 2.

Leveraging the predictive \mathcal{V} -information, the predictive heterogeneity defined in Equation 10 characterizes the *maximal additional information* that can be used by the prediction model when involving the environment variable \mathcal{E} . It restricts the prediction models in \mathcal{V} and the explored additional information could benefit the prediction performance of the model $f \in \mathcal{V}$, for which it is named predictive heterogeneity. Next, we present some basic properties of the interaction heterogeneity and predictive heterogeneity.

Proposition 6 (Basic Properties of Predictive Heterogeneity) *Let X, Y be random variables taking values in $\mathcal{X} \times \mathcal{Y}$, \mathcal{V} be a function family, and $\mathcal{E}, \mathcal{E}_1, \mathcal{E}_2$ be environment sets.*

1. Monotonicity: *If $\mathcal{E}_1 \subseteq \mathcal{E}_2$, $\mathcal{H}_{\mathcal{V}}^{\mathcal{E}_1}(X \rightarrow Y) \leq \mathcal{H}_{\mathcal{V}}^{\mathcal{E}_2}(X \rightarrow Y)$.*
2. Nonnegativity: *$\mathcal{H}_{\mathcal{V}}^{\mathcal{E}}(X \rightarrow Y) \geq 0$.*
3. Boundedness: *For discrete Y , $\mathcal{H}_{\mathcal{V}}^{\mathcal{E}}(X \rightarrow Y) \leq H_{\mathcal{V}}(Y|X)$.*
4. Corner Case: *If the predictive family \mathcal{V} is the largest possible predictive family that includes all possible models, i.e. $\mathcal{V} = \Omega$, we have $\mathcal{H}^{\mathcal{E}}(X, Y) = \mathcal{H}_{\Omega}^{\mathcal{E}}(X \rightarrow Y)$.*

Proofs can be found at Appendix A. For further theoretical properties of predictive heterogeneity, in Section 3.3, we derive its explicit forms under *endogeneity*, a common reflection of data heterogeneity. And we demonstrate in Section 3.4 that our proposed predictive heterogeneity can be empirically estimated with guarantees if the complexity of \mathcal{V} is bounded (e.g., its Rademacher complexity).

3.3 Theoretical Properties in Linear Cases

In this section, we conduct a theoretical analysis of the predictive heterogeneity in multiple linear settings. Specifically, we consider two scenarios: (1) a homogeneous case with independent noises and (2) heterogeneous cases with endogeneity arising from selection bias and hidden variables. By examining these typical settings, we approximate the analytical forms of the proposed measure and draw insightful conclusions that can be generalized to more complex scenarios.

Firstly, under a homogeneous case with no data heterogeneity, Theorem 7 proves that our measure is bounded by the scale of label noises (which is usually small) and reduces to 0 in linear case under mild assumptions. It indicates that the predictive heterogeneity is insensitive to independent noises. Notably that in the linear case we only deal with the environment variable satisfying $X \perp \epsilon|\mathcal{E}$, since in common prediction tasks, the independent noises are unknown and unrealistic to be exploited for the prediction.

Theorem 7 (Homogeneous Case with Independent Noises) *For a prediction task $X \rightarrow Y$ where X, Y are random variables taking values in $\mathbb{R}^n \times \mathbb{R}$, consider the data generation process as $Y = g(x) + \epsilon, \epsilon \sim \mathcal{N}(0, \sigma^2)$ where $g : \mathbb{R}^n \rightarrow \mathbb{R}$ is a measurable function. 1) For a function class \mathcal{G} such that $g \in \mathcal{G}$, define the function family as $\mathcal{V}_{\mathcal{G}} = \{f|f[x] = \mathcal{N}(\phi(x), \sigma_V^2), \phi \in \mathcal{G}, \sigma_V \in \mathbb{R}^+\}$. With an environment set \mathcal{E} , we have $\mathcal{H}_{\mathcal{V}_{\mathcal{G}}}^{\mathcal{E}}(X \rightarrow Y) \leq \pi\sigma^2$. 2) Take $n = 1$ and $g(x) = \beta x, \beta \in \mathbb{R}$. Without loss of generality, assume $\mathbb{E}[X] = 0$ and $\mathbb{E}[X^2]$ exists. Given the function family $\mathcal{V}_{\sigma} = \{f|f[x] = \mathcal{N}(\theta x, \sigma^2), \theta \in \mathbb{R}, \sigma \text{ fixed}\}$ and the environment set $\mathcal{E} = \{\mathcal{E}|\mathcal{E} \in \mathcal{C}, |\text{supp}(\mathcal{E})| = 2, X \perp \epsilon|\mathcal{E}\}$. We have $\mathcal{H}_{\mathcal{V}_{\sigma}}^{\mathcal{E}}(X \rightarrow Y) = 0$. Proofs can be found at Appendix B.*

Secondly, we examine the proposed measure under *two typical cases of data heterogeneity* (Fan et al., 2014), named *endogeneity by selection bias* (Heckman, 1979; Winship and Mare, 1992; Cui and Athey, 2022) and *endogeneity with hidden variables* (Fan et al., 2014; Arjovsky et al., 2019).

To begin with, in Theorem 8, we consider the prediction task $X \rightarrow Y$ with X, Y taking values in $\mathbb{R}^2 \times \mathbb{R}$. Let $X = [S, V]^T$. The predictive family is specified as:

$$\mathcal{V} = \{f|f[x] = \mathcal{N}(\theta_S S + \theta_V V, \sigma^2), \quad \theta_S, \theta_V \in \mathbb{R}, \sigma = 1\}. \quad (11)$$

And the data distribution $P(X, Y)$ is a mixture of latent sub-populations, which could be formulated by an environment variable $\mathcal{E}^* \in \mathcal{C}$ such that $P(X, Y) = \sum_{e \in \text{supp}(\mathcal{E}^*)} P(\mathcal{E}^* = e)P(X, Y|\mathcal{E}^* = e)$. For each $e \in \text{supp}(\mathcal{E}^*)$, $P(X, Y|\mathcal{E}^* = e)$ is the distribution of a homogeneous sub-population. Note that the prediction task is to predict Y with covariates X , and the sub-population structure is latent. That is, $P(\mathcal{E}^*|X, Y)$ is *unknown* for models. In the following, we derive the analytical forms of our measure under the one typical case.

Theorem 8 (Endogeneity with Selection Bias) *For the prediction task $X = [S, V]^T \rightarrow Y$ with a latent environment variable \mathcal{E}^* , the data generation process with selection bias is defined as:*

$$Y = \beta S + f(S) + \epsilon_Y, \epsilon_Y \sim \mathcal{N}(0, \sigma_Y^2); \quad V = r(\mathcal{E}^*)f(S) + \sigma(\mathcal{E}^*) \cdot \epsilon_V, \epsilon_V \sim \mathcal{N}(0, 1), \quad (12)$$

where $f : \mathbb{R} \rightarrow \mathbb{R}$ and $r, \sigma : \text{supp}(\mathcal{E}^*) \rightarrow \mathbb{R}$ are measurable functions. $\beta \in \mathbb{R}$. Assume that $\mathbb{E}[S^2]$ is finite, $\mathbb{E}[f(S)S] = 0$ and there exists $L > 1$ such that $L\sigma^2(\mathcal{E}^*) < r^2(\mathcal{E}^*)\mathbb{E}[f^2]$. For the predictive family defined in equation 11 and the environment set $\mathcal{E} = \mathcal{C}$, the predictive heterogeneity of the prediction task $[S, V]^T \rightarrow Y$ approximates to:

$$\mathcal{H}_V^{\mathcal{C}}(X \rightarrow Y) \approx \frac{\text{Var}(r_e)\mathbb{E}[f^2] + \mathbb{E}[\sigma^2(\mathcal{E}^*)]}{\mathbb{E}[r_e^2]\mathbb{E}[f^2] + \mathbb{E}[\sigma^2(\mathcal{E}^*)]}\mathbb{E}[f^2(S)], \text{ error bounded by } \frac{1}{2} \max(\sigma_Y^2, R(r, \sigma, f)). \quad (13)$$

And further we have

$$\begin{aligned} R(r(\mathcal{E}^*), \sigma(\mathcal{E}^*), f) &= \mathbb{E}\left[\left(\frac{1}{\frac{r^2\mathbb{E}[f^2]}{\sigma^2} + 1}\right)^2\mathbb{E}[f^2] + \mathbb{E}_{\mathcal{E}^*}\left[\left(\frac{1}{\frac{r}{\sigma} + \frac{\sigma}{r\mathbb{E}[f^2]}}\right)^2\right]\right] \\ &< \mathbb{E}[f^2]\left(\frac{1}{(L+1)^2} + \frac{1}{L+2+\frac{1}{L}}\right). \end{aligned} \quad (14)$$

Proofs can be found at Appendix C.

Intuitively, the data generation process in Theorem 8 introduces the spurious correlation between the spurious feature V and the target Y , which varies across different sub-populations (i.e. $r(\mathcal{E}^*)$ and $\sigma(\mathcal{E}^*)$ varies) and brings about data heterogeneity. Here $\mathbb{E}[f(S)S] = 0$ indicates a model misspecification since there is a nonlinear term $f(S)$ that could not be inferred by the linear predictive family with the stable feature S . The constant L characterizes the strength of the spurious correlation between V and Y . Larger L means V could provide more information for prediction.

From the approximation in Equation 13, we can see that our proposed predictive heterogeneity is dominated by two terms: (1) $\text{Var}[r(\mathcal{E}^*)]/\mathbb{E}[r^2(\mathcal{E}^*)]$ characterizes the variance of $r(\mathcal{E}^*)$ among sub-populations; (2) $\mathbb{E}[f^2(S)]$ reflects the strength of model misspecifications. These two components account for two sources of the data heterogeneity under selection bias, which validates the rationality of our proposed measure. Based on the theorem, it can be inferred that the degree of predictive heterogeneity increases with greater variability of $r(\mathcal{E}^*)$ among sub-populations and stronger model misspecifications. In other words, when the sub-populations differ significantly from each other and the model is not accurately specified, the predictive heterogeneity is likely to be larger.

Additionally, in Theorem 9, we analyze our measure under endogeneity with hidden variables. In Theorem 9, an anti-causal covariate V is generated via the causal diagram

like $Y \rightarrow V \leftarrow \mathcal{E}^*$ with a hidden environment variable \mathcal{E}^* . However, since \mathcal{E}^* is omitted from the prediction models, the relationship between V and Y is biased, which inhibits the prediction power.

Theorem 9 (Endogeneity with Hidden Variables) *For the prediction task $[S, V]^T \rightarrow Y$ with a latent environment variable \mathcal{E}^* , the data generation process with hidden variables is defined as:*

$$Y = \beta S + f(S) + \epsilon_Y, \epsilon_Y \sim \mathcal{N}(0, \sigma_Y^2); \quad V = r(\mathcal{E}^*)(f(S) + \epsilon_Y) + \sigma(\mathcal{E}^*)\epsilon_V, \epsilon_V \sim \mathcal{N}(0, 1), \quad (15)$$

where $f : \mathbb{R} \rightarrow \mathbb{R}$ and $r, \sigma : \text{supp}(\mathcal{E}^*) \rightarrow \mathbb{R}$ are measurable functions. $\beta \in \mathbb{R}$. Assume that $\mathbb{E}[f(S)S] = 0$ and there exists $L > 1$ such that $L\sigma^2(\mathcal{E}^*) < r^2(\mathcal{E}^*)(\mathbb{E}[f^2] + \sigma_Y^2)$. For the predictive family defined in equation 11 and the environment set $\mathcal{E} = \mathcal{C}$, the predictive heterogeneity of the prediction task $[S, V]^T \rightarrow Y$ approximates to:

$$\begin{aligned} \mathcal{H}_Y^{\mathcal{C}}(X \rightarrow Y) &\approx \frac{\text{Var}(r_e)(\mathbb{E}[f^2] + \sigma_Y^2) + \mathbb{E}[\sigma^2(\mathcal{E}^*)]}{\mathbb{E}[r_e^2](\mathbb{E}[f^2] + \sigma_Y^2) + \mathbb{E}[\sigma^2(\mathcal{E}^*)]} (\mathbb{E}[f^2(S)] + \sigma_Y^2), \\ \text{error bounded by } &\frac{1}{2} \max(\sigma_Y^2, R(r, \sigma, f)). \end{aligned} \quad (16)$$

And further we have:

$$\begin{aligned} R(r(\mathcal{E}^*), \sigma(\mathcal{E}^*), f) &= \mathbb{E}\left[\left(\frac{1}{r^2(\mathbb{E}[f^2] + \sigma_Y^2) + 1}\right)^2\right] (\mathbb{E}[f^2] + \sigma_Y^2) + \mathbb{E}_{\mathcal{E}^*}\left[\left(\frac{1}{\frac{r}{\sigma} + \frac{\sigma}{r(\mathbb{E}[f^2] + \sigma_Y^2)}}\right)^2\right] \\ &< (\mathbb{E}[f^2] + \sigma_Y^2) \left(\frac{1}{(L+1)^2} + \frac{1}{L+2+\frac{1}{L}}\right). \end{aligned} \quad (17)$$

Proofs can be found at Appendix C.

Intuitively, the data generation process in Theorem 9 introduces the *biased* anti-causal relationship between the spurious feature V and the target Y , which varies across different sub-populations (i.e. $r(\mathcal{E}^*)$ and $\sigma(\mathcal{E}^*)$ varies) and brings about data heterogeneity. Here, similar as Theorem 8, $\mathbb{E}[f(S)S] = 0$ indicates model misspecification and the constant L characterizes the strength of the biased anti-causal relationship between V and Y , where larger L means more information that V could provide for predicting Y when \mathcal{E}^* is missing. From the approximation in Equation 16, we can see that our proposed predictive heterogeneity is dominated by two terms: (1) $\text{Var}[r(\mathcal{E}^*)]/\mathbb{E}[r^2(\mathcal{E}^*)]$ characterizes the variance of $r(\mathcal{E}^*)$ among sub-populations; (2) $\mathbb{E}[f^2(S)] + \sigma_Y^2$ reflects the maximal additional information that could be provided by V .

In the broader context, Theorem 1, 2, and 3 suggest that our proposed predictive heterogeneity measure is equipped with remarkable properties, namely its insensitivity to homogeneous cases and its ability to account for the latent heterogeneity arising from typical sources of data heterogeneity. These findings highlight the effectiveness of our measure in accurately characterizing predictive heterogeneity in various machine learning tasks.

3.4 PAC Guarantees for Predictive Heterogeneity Estimation

Defined under explicit computation constraints, our Predictive Heterogeneity could be empirically estimated with guarantees if the complexity of the model family \mathcal{V} is bounded. In

this work, we provide finite sample generalization bounds with the Rademacher complexity. First, we describe the definition of the empirical predictive heterogeneity, the explicit formula for which could be found in Definition 10.

The dataset $\mathcal{D} = \{(x_i, y_i)\}_{i=1}^{|\mathcal{D}|}$ is independently and identically drawn from the population X, Y . Given a function family \mathcal{V} and an environment set \mathcal{E}_K such that for $\mathcal{E} \in \mathcal{E}_K$, $\text{supp}(\mathcal{E}) = \{(e_k)_{k=1}^K\}$, let \mathcal{Q} be the set of all probability distributions of X, Y, \mathcal{E} where $\mathcal{E} \in \mathcal{E}_K$. The empirical predictive heterogeneity $\hat{\mathcal{H}}_{\mathcal{V}}^{\mathcal{E}_K}(X \rightarrow Y; \mathcal{D})$ is given by:

$$\hat{\mathcal{H}}_{\mathcal{V}}^{\mathcal{E}_K}(X \rightarrow Y; \mathcal{D}) = \sup_{\mathcal{E} \in \mathcal{E}_K} \hat{\mathbb{I}}_{\mathcal{V}}(X \rightarrow Y | \mathcal{E}; \mathcal{D}) - \hat{\mathbb{I}}_{\mathcal{V}}(X \rightarrow Y; \mathcal{D}) \quad (18)$$

$$= \sup_{\hat{Q} \in \mathcal{Q}} \sum_{k=1}^K \left[\hat{Q}(\mathcal{E} = e_k) \hat{H}_{\mathcal{V}}(Y | \mathcal{E} = e_k; \mathcal{D}) - \hat{Q}(\mathcal{E} = e_k) \hat{H}_{\mathcal{V}}(Y | X, \mathcal{E} = e_k; \mathcal{D}) \right] \quad (19)$$

$$- [\hat{H}_{\mathcal{V}}(Y; \mathcal{D}) - \hat{H}_{\mathcal{V}}(Y | X; \mathcal{D})]. \quad (20)$$

Specifically,

$$\hat{Q}(\mathcal{E} = e_k) \hat{H}_{\mathcal{V}}(Y | X, \mathcal{E} = e_k; \mathcal{D}) \quad (21)$$

$$= \inf_{f \in \mathcal{V}} \hat{Q}(\mathcal{E} = e_k) \sum_{x_i, y_i \in \mathcal{D}} -\log f[x_i](y_i) \frac{\hat{Q}(x_i, y_i | \mathcal{E} = e_k)}{\sum_{x_j, y_j \in \mathcal{D}} \hat{Q}(x_j, y_j | \mathcal{E} = e_k)} \quad (22)$$

$$= \inf_{f \in \mathcal{V}} \hat{Q}(\mathcal{E} = e_k) \sum_{x_i, y_i \in \mathcal{D}} -\log f[x_i](y_i) \frac{\hat{Q}(\mathcal{E} = e_k | x_i, y_i) \hat{Q}(x_i, y_i)}{\sum_{x_j, y_j \in \mathcal{D}} \hat{Q}(\mathcal{E} = e_k | x_j, y_j) \hat{Q}(x_j, y_j)} \quad (23)$$

$$= \inf_{f \in \mathcal{V}} \hat{Q}(\mathcal{E} = e_k) \sum_{x_i, y_i \in \mathcal{D}} -\log f[x_i](y_i) \frac{\hat{Q}(\mathcal{E} = e_k | x_i, y_i) \hat{Q}(x_i, y_i)}{\hat{Q}(\mathcal{E} = e_k)} \quad (24)$$

$$= \inf_{f \in \mathcal{V}} \sum_{x_i, y_i \in \mathcal{D}} -\log f[x_i](y_i) \hat{Q}(\mathcal{E} = e_k | x_i, y_i) \hat{Q}(x_i, y_i) \quad (25)$$

$$= \inf_{f \in \mathcal{V}} \frac{1}{|\mathcal{D}|} \sum_{x_i, y_i \in \mathcal{D}} -\log f[x_i](y_i) \hat{Q}(\mathcal{E} = e_k | x_i, y_i). \quad (26)$$

The explicit formula for $\hat{Q}(\mathcal{E} = e_k) \hat{H}_{\mathcal{V}}(Y | \mathcal{E} = e_k; \mathcal{D})$, $\hat{H}_{\mathcal{V}}(Y | X; \mathcal{D})$ and $\hat{H}_{\mathcal{V}}(Y; \mathcal{D})$ could be similarly derived. Here we are ready to formally define the empirical predictive heterogeneity.

Definition 10 (Empirical Predictive Heterogeneity) *For the prediction task $X \rightarrow Y$ with X, Y taking values in $\mathcal{X} \times \mathcal{Y}$, a dataset \mathcal{D} is independently and identically drawn from the population such that $\mathcal{D} = \{(x_i, y_i)\}_{i=1}^N \sim X, Y$. Given the predictive family \mathcal{V} and the environment set $\mathcal{E}_K = \{\mathcal{E} | \mathcal{E} \in \mathcal{C}, |\text{supp}(\mathcal{E})| = K\}$ where $K \in \mathbb{N}$. Without loss of generality, we specify that $\text{supp}(\mathcal{E}) = \{(e_k)_{k=1}^K\}$ where e_k denotes a single environment. Let \mathcal{Q} be the set of all probability distributions of X, Y, \mathcal{E} where $\mathcal{E} \in \mathcal{E}_K$. The empirical predictive heterogeneity $\hat{\mathcal{H}}_{\mathcal{V}}^{\mathcal{E}_K}(X \rightarrow Y; \mathcal{D})$ with respect to \mathcal{D} is defined as:*

$$\hat{\mathcal{H}}_{\mathcal{V}}^{\mathcal{E}_K}(X \rightarrow Y; \mathcal{D}) = \sup_{\hat{Q} \in \mathcal{Q}} \sum_{k=1}^K \left[\hat{Q}(\mathcal{E} = e_k) \hat{H}_{\mathcal{V}}(Y | \mathcal{E} = e_k; \mathcal{D}) - \hat{Q}(\mathcal{E} = e_k) \hat{H}_{\mathcal{V}}(Y | X, \mathcal{E} = e_k; \mathcal{D}) \right] - [\hat{H}_{\mathcal{V}}(Y; \mathcal{D}) - \hat{H}_{\mathcal{V}}(Y | X; \mathcal{D})], \quad (27)$$

where

$$\hat{Q}(\mathcal{E} = e_k) \hat{H}_{\mathcal{V}}(Y|X, \mathcal{E} = e_k; \mathcal{D}) = \inf_{f \in \mathcal{V}} \frac{1}{|\mathcal{D}|} \sum_{x_i, y_i \in \mathcal{D}} -\log f[x_i](y_i) \hat{Q}(\mathcal{E} = e_k | x_i, y_i). \quad (28)$$

$$\hat{Q}(\mathcal{E} = e_k) \hat{H}_{\mathcal{V}}(Y|\mathcal{E} = e_k; \mathcal{D}) = \inf_{f \in \mathcal{V}} \frac{1}{|\mathcal{D}|} \sum_{x_i, y_i \in \mathcal{D}} -\log f[\emptyset](y_i) \hat{Q}(\mathcal{E} = e_k | x_i, y_i). \quad (29)$$

$$\hat{H}_{\mathcal{V}}(Y|X; \mathcal{D}) = \inf_{f \in \mathcal{V}} \frac{1}{|\mathcal{D}|} \sum_{x_i, y_i \in \mathcal{D}} -\log f[x_i](y_i). \quad (30)$$

$$\hat{H}_{\mathcal{V}}(Y; \mathcal{D}) = \inf_{f \in \mathcal{V}} \frac{1}{|\mathcal{D}|} \sum_{x_i, y_i \in \mathcal{D}} -\log f[\emptyset](y_i). \quad (31)$$

Then we give the PAC bound over the empirical usable predictive heterogeneity in Theorem 11.

Theorem 11 (PAC Bound) *Consider the prediction task $X \rightarrow Y$ where X, Y are random variables taking values in $\mathcal{X} \times \mathcal{Y}$. Assume that the predictive family \mathcal{V} satisfies $\forall x \in \mathcal{X}, \forall y \in \mathcal{Y}, \forall f \in \mathcal{V}, \log f[x](y) \in [-B, B]$ where $B > 0$. For given $K \in \mathbb{N}$, the environment set is defined as $\mathcal{E}_K = \{\mathcal{E} | \mathcal{E} \in \mathcal{C}, |\text{supp}(\mathcal{E})| = K\}$ where $K \in \mathbb{N}$. Without loss of generality, we specify that $\text{supp}(\mathcal{E}) = \{(e_k)_{k=1}^K\}$ where e_k denotes a single environment. Let \mathcal{Q} be the set of all probability distributions of X, Y, \mathcal{E} where $\mathcal{E} \in \mathcal{E}_K$. Take an $e \in \text{supp}(\mathcal{E})$ and define a function class $\mathcal{G} = \{g | g(x, y) = \log f[x](y) Q(\mathcal{E} = e | x, y), f \in \mathcal{V}, Q \in \mathcal{Q}\}$. Denote the Rademacher complexity of \mathcal{G} with N samples by $\mathcal{R}_N(\mathcal{G})$. Then for any $\delta \in (0, 1/(2K + 2))$, with a probability over $1 - 2(K + 1)\delta$, for dataset \mathcal{D} independently and identically drawn from X, Y , we have:*

$$|\mathcal{H}_{\mathcal{V}}^{\mathcal{E}_K}(X \rightarrow Y) - \hat{\mathcal{H}}_{\mathcal{V}}^{\mathcal{E}_K}(X \rightarrow Y; \mathcal{D})| \leq 4(K + 1) \mathcal{R}_{|\mathcal{D}|}(\mathcal{G}_{\mathcal{V}}) + 2(K + 1)B \sqrt{2 \log \frac{1}{\delta} / |\mathcal{D}|}, \quad (32)$$

where $\mathcal{R}_{|\mathcal{D}|}(\mathcal{G}_{\mathcal{V}}) = \mathcal{O}(|\mathcal{D}|^{-\frac{1}{2}})$ (Bartlett and Mendelson, 2002). Proofs can be found at Appendix D.

4 Algorithm

To empirically estimate the predictive heterogeneity in Definition 10, we derive the Information Maximization (IM) algorithm from the formal definition in Equation 27 to infer the distribution of \mathcal{E} that maximizes the empirical predictive heterogeneity $\hat{\mathcal{H}}_{\mathcal{V}}^{\mathcal{E}_K}(X \rightarrow Y; \mathcal{D})$.

Objective Function. Given dataset $\mathcal{D} = \{X_N, Y_N\} = \{(x_i, y_i)\}_{i=1}^N$, denote $\text{supp}(\mathcal{E}) = \{e_1, \dots, e_K\}$, we parameterize the distribution of $\mathcal{E} | (X_N, Y_N)$ with weight matrix $W \in \mathcal{W}_K$, where K is the pre-defined number of environments and $\mathcal{W}_K = \{W : W \in \mathbb{R}_+^{N \times K} \text{ and } W \mathbf{1}_K = \mathbf{1}_N\}$ is the allowed weight space. Each element w_{ij} in W represents $P(\mathcal{E} = e_j | x_i, y_i)$ (the probability of the i -th data point belonging to the j -th sub-population). For a predictive family \mathcal{V} , the solution to the supremum problem in the Definition 10 is equivalent to the following objective function:

$$\begin{aligned} \min_{W \in \mathcal{W}_K} \mathcal{R}_{\mathcal{V}}(W, \theta_1^*(W), \dots, \theta_K^*(W)) &= \left\{ \frac{1}{N} \sum_{i=1}^N \sum_{j=1}^K w_{ij} \ell_{\mathcal{V}}(f_{\theta_j^*}(x_i), y_i) + U_{\mathcal{V}}(W, Y_N) \right\}, \\ \text{s.t. } \theta_j^*(W) &\in \arg \min_{\theta} \left\{ \mathcal{L}_{\mathcal{V}}^j(W, \theta) = \sum_{i=1}^N w_{ij} \ell_{\mathcal{V}}(f_{\theta}(x_i), y_i) \right\}, \quad \text{for } j = 1, \dots, K, \end{aligned} \quad (33)$$

where $f_\theta : \mathcal{X} \rightarrow \mathcal{Y}$ denotes a predicting function parameterized by θ , $\ell_{\mathcal{V}}(\cdot, \cdot) : \mathcal{Y} \times \mathcal{Y} \rightarrow \mathbb{R}$ represents a loss function and $U_{\mathcal{V}}(W, Y_N)$ is a regularizer. Specifically, f_θ , $\ell_{\mathcal{V}}$ and $U_{\mathcal{V}}$ are determined by the predictive family \mathcal{V} . Here we provide implementations for two typical and general machine learning tasks, regression and classification.

4.1 Regression

For the *regression task*, the predictive family is typically modeled as:

$$\mathcal{V}_1 = \{g : g[x] = \mathcal{N}(f_\theta(x), \sigma^2), f \text{ is the predicting function and } \theta \text{ is learnable, } \sigma \text{ is a constant}\}. \quad (34)$$

The corresponding loss function is $\ell_{\mathcal{V}_1}(f_\theta(X), Y) = (f_\theta(X) - Y)^2$, and $U_{\mathcal{V}_1}(W, Y_N)$ becomes

$$U_{\mathcal{V}_1}(W, Y_N) = \text{Var}_{j \in [K]}(\overline{Y_N^j}) = \sum_{j=1}^K \left(\sum_{i=1}^N w_{ij} y_i \right)^2 \frac{1}{N \sum_{i=1}^N w_{ij}} - \left(\frac{1}{N} \sum_{i=1}^N y_i \right)^2 \quad (35)$$

where $\overline{Y_N^j}$ denotes the mean value of the label Y given $\mathcal{E} = e_j$ and $U(W, Y_N)$ calculates the variance of $\overline{Y_N^j}$ among sub-populations $e_1 \sim e_K$.

4.2 Classification

For the *classification task*, the predictive family is typically modeled as:

$$\mathcal{V}_2 = \{g : g[x] = f_\theta(x) \in \Delta_c, f \text{ is the classification model and } \theta \text{ is learnable}\}, \quad (36)$$

where c is the class number and Δ_c denotes the c -dimensional simplex. Here each model in the predictive family \mathcal{V}_2 outputs a discrete distribution in the form of a c -dimensional simplex. In this case, the corresponding loss function $\ell_{\mathcal{V}_2}(\cdot, \cdot)$ is the cross entropy loss and the regularizer becomes $U_{\mathcal{V}_2}(W, Y_N) = -\sum_{j=1}^K \frac{1}{N} (\sum_{i=1}^N w_{ij}) H(Y_N^j)$, where $H(Y_N^j)$ is the entropy of Y given $\mathcal{E} = e_j$.

4.3 Optimization.

The bi-level optimization in Equation 33 can be solved by performing projected gradient descent w.r.t. W . The gradient of W can be calculated by: (we omit the subscript \mathcal{V} here)

$$\nabla_W \mathcal{R} = \nabla_W U + [\ell(f_{\theta_j}(x_i), y_i)]_{i,j}^{N \times K} + \sum_{j=1}^K \boxed{\nabla_{\theta_j} \mathcal{R} |_{\theta_j^*} \nabla_W \theta_j^*}, \quad (37)$$

$$\text{where } \boxed{\nabla_{\theta_j} \mathcal{R} |_{\theta_j^*} \nabla_W \theta_j^*} \approx \nabla_{\theta_j} \mathcal{R} |_{\theta_j^t} \sum_{h \leq t} \left[\prod_{k < h} \left(I - \frac{\partial^2 \mathcal{L}^j}{\partial \theta_j \partial \theta_j^T} \Big|_{\theta_j^{t-k-1}} \right) \right] \frac{\partial^2 \mathcal{L}^j}{\partial \theta_j \partial W^T} \Big|_{\theta_j^{t-h-1}} \quad (38)$$

$$\approx \nabla_{\theta_j} \mathcal{R} |_{\theta_j^t} \frac{\partial^2 \mathcal{L}^j}{\partial \theta_j \partial W^T} \Big|_{\theta_j^{t-1}}, \text{ for } j = 1, \dots, K. \quad (39)$$

where $[\ell(f_{\theta_j}(x_i), y_i)]_{i,j}^{N \times K}$ is an $N \times K$ matrix in which the (i, j) -th element is $\ell(f_{\theta_j}(x_i), y_i)$. Here Equation 38 approximates θ_j^* by θ_j^t from t steps of inner loop gradient descent and Equation 39 takes $t = 1$ and performs *1-step truncated backpropagation* (Shaban et al.,

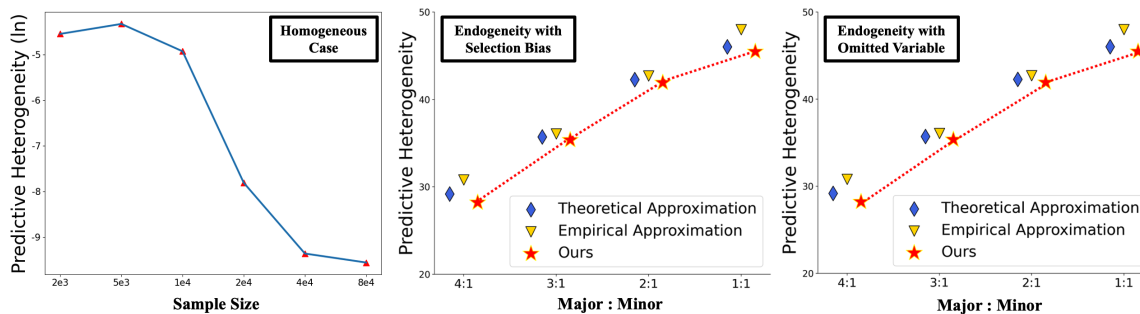


Figure 1: Numerical results of the toy examples in Section 3.3. The left sub-figure plots the estimated predictive heterogeneity under the setting of Theorem 7, the middle sub-figure plots the theoretical approximation, empirical approximation and our results under the setting of Theorem 8, and the right one is under the setting of Theorem 9.

2019; Zhou et al., 2022). Our information maximization algorithm updates W by projected gradient descent as:

$$W \leftarrow \text{Proj}_{\mathcal{W}_K}(W - \eta \nabla_W \mathcal{R}), \quad \eta \text{ is the learning rate of } W. \quad (40)$$

Then we prove that minimizing Equation 33 exactly finds the supremum w.r.t. \mathcal{E} in the Definition 10 (formal) of the empirical predictive heterogeneity.

Theorem 12 (Justification of the IM Algorithm) *For the regression task with predictive family \mathcal{V}_1 and classification task with \mathcal{V}_2 , the optimization of Equation 33 is equivalent to the supremum problem of the empirical predictive heterogeneity $\hat{\mathcal{H}}_{\mathcal{V}_1}^{\mathcal{E}_K}(X \rightarrow Y; \mathcal{D})$, $\hat{\mathcal{H}}_{\mathcal{V}_2}^{\mathcal{E}_K}(X \rightarrow Y; \mathcal{D})$ respectively in Equation 27 with the pre-defined environment number K (i.e. $|\text{supp}(\mathcal{E})| = K$). Proofs can be found at Appendix E.*

Remark 13 (Difference from Expectation Maximization) *The expectation maximization (EM) algorithm is to infer latent variables of a statistic model to achieve the **maximum likelihood**. Our proposed information maximization (IM) algorithm is to infer the latent variables W which brings the **maximal predictive heterogeneity** associated with the maximal information. Due to the regularizer $U_{\mathcal{V}}$ in our objective function, the EM algorithm cannot efficiently solve our problem, and therefore we adopt bi-level optimization techniques.*

4.4 Approximation Accuracy

Here we provide some additional numerical results of our linear examples in Section 3.3. In the left sub-figure of Figure 1, we plot the estimated predictive heterogeneity under the setting of Theorem 7 where the analytical solution is equal to 0. From the results, we can see that with the growing of sample size, the estimated value of our IM algorithm is approaching to 0 (note that the y -axis is $\ln(\text{estimated value})$). In the middle sub-figure, for the setting in Theorem 8, we plot the theoretical approximation, empirical approximation (finite sample case) and the estimated value of the predictive heterogeneity under different ratios between the majority and the minority (which controls the $\text{Var}[r(\mathcal{E}^*)]$ in Equation 13). And the

right sub-figure plots the same values under the setting in Theorem 9. From these two figures, we can see that (1) the empirical approximation under finite samples lies closely to the theoretical approximation, which is supported by our generalization bounds in Theorem 11; (2) the estimated value of our IM algorithm is closely to the theoretical approximation,, which demonstrates the accuracy of our approximation algorithm in Equation 38 and 39. Also, as the ratio changes from 4 : 1 to 1 : 1, the data heterogeneity is increasing, and our predictive heterogeneity is also increasing, which is controlled by the term $\text{Var}(r(\mathcal{E}^*))$ in Equation 13 and 16.

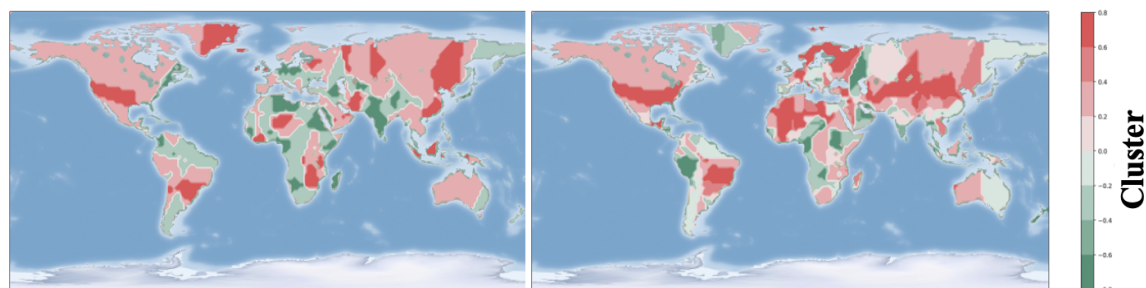
5 Experiments

5.1 Reveal Explainable Sub-population Structures

The predictive heterogeneity could provide valuable insights for the sub-population division and support decision-making across various fields, including agricultural and sociological research, as well as object recognition. Our illustrative examples below reveal that the learned sub-population divisions are highly explainable and relevant for decision-making purposes.

Example: Agriculture It is known that the climate affects crop yields and crop suitability (Lobell et al., 2008). We utilize the data from the NOAA database which contains daily weather from weather stations around the world. Following Zhao et al. (2021), we extracted summary statistics from the weather sequence of the year 2018, including the average yearly temperature, humidity, wind speed and rainy days. The task is to predict the *crop yield* in each place with *weather summary statistics* and *location covariates* (*i.e. longitude and latitude*) of the place. For easy illustration, we focus on the places with crop types of wheat or rice. Notably, our input covariates do *not* contain the crop type information. We use MLP models in this task and set $K = 2$ for our IM algorithm.

Given that crop yield prediction mechanisms are closely related to crop type, which is unknown in the prediction task, we believe this causes data heterogeneity in the entire dataset, and the recognized predictive heterogeneity should relate to it. To demonstrate the rationality of our measure, we plot the real distribution map of wheat and rice planting areas in Figure 2(a) and the learned two sub-populations of our IM algorithm in Figure



(a) Division of wheat and rice cultivation areas

(b) Division learned by our algorithm

Figure 2: Results on the crop yield data. We color each region according to its main crop type, and the shade represents the proportion of the main crop type after smoothing via k -means ($k = 3$).

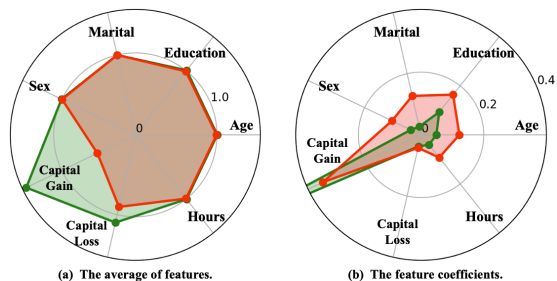


Figure 3: Results on the Adults data. Here we show the average of features and the feature coefficients of the two learned sub-populations.

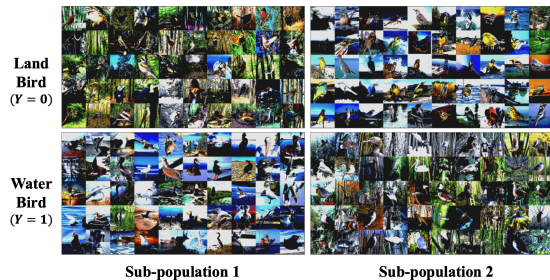


Figure 4: Results on the Waterbird data. Here we *randomly sample* 50 images for each class and each learned sub-population.

2(b). The division given by our algorithm is quite similar to the real division of the two crops, indicating the rationality of our measure. We observe some discrepancies in areas such as the Tibet Plateau in Asia, which we attribute to the absence of significant features such as population density and altitude that significantly affect crop yields.

Example: Sociology We use the UCI Adult dataset (Kohavi and Becker, 1996), which is widely used in the study of algorithmic fairness and derived from the 1994 Current Population Survey conducted by the US Census Bureau. The task is to predict whether the income of a person is greater or less than 50k US dollars based on personal features. We use linear models in this task and set $K = 2$. In this example, we aim to investigate whether *sub-population structures* within data affect the learning of machine learning models.

In Figure 3 (a), we plot summary statistics for the two sub-populations, revealing a key difference in capital gain. In Figure 3 (b), we present the feature importance given by linear models for the two sub-populations, and find that for individuals with high capital gain, the prediction model mainly relies on capital gain, which is fair. However, for individuals with low capital gain, models also consider sensitive attributes such as sex and marital status, which have been known to cause discrimination. Our results are consistent with those found in (Zhao et al., 2021) and can help identify potential inequalities in decision-making. For example, our findings suggest potential discrimination towards individuals with low capital gain, which could motivate algorithmic design and improve policy fairness.

Example: Object Recognition Finally, we utilize the Waterbird dataset (Sagawa et al., 2019), which is widely used as a benchmark in the field of robust learning, to investigate the impact of spurious correlations on machine learning models. The task is to recognize waterbirds or landbirds, but the images contain *spurious correlations* between the background and the target label. For the majority of images, waterbirds are located on water and landbirds on land, whereas for a minority of images, this correlation is reversed. Therefore, the spurious correlation leads to predictive heterogeneity in this dataset, which could significantly affect the performance of machine learning models. In this example, we use the ResNet18 and set $K = 2$ in our IM algorithm.

Our method successfully captures the spurious correlation and identifies two sub-populations of images with inverse correlations between the object and the background. To demonstrate the effectiveness of our method, we randomly sample 50 images for each class and each learned sub-population and plot them in Figure 4. In sub-population 1, the majority of

landbirds are on the ground and waterbirds are in the water, while in sub-population 2, the majority of landbirds are in the water and waterbirds are on the ground. Our findings suggest that the proposed approach can be leveraged by robust learning methods (Sagawa et al., 2019; Koyama and Yamaguchi, 2020) to improve the generalization ability of machine learning models. By eliminating the influence of spurious correlations, our method could significantly enhance the robustness and reliability of machine learning models. Overall, our study highlights the importance of addressing predictive heterogeneity in image classification tasks and provides a practical solution for achieving robust learning performance.

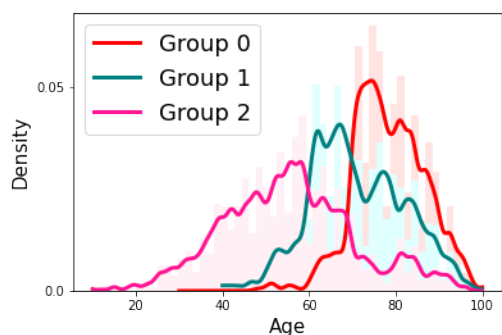


Figure 5: Results on the COVID-19 data. We plot the age distributions of dead people ($Y = 1$) in each learned subgroup.

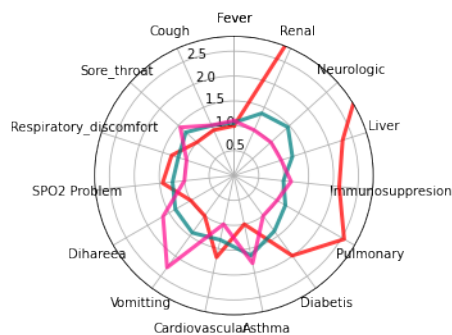


Figure 6: Results on the COVID-19 data. We show the averages of typical features of dead people ($Y = 1$) in each learned subgroup.

5.2 Assist Scientific Discovery: Uncover Factors Related to Mortality

In order to fully demonstrate the efficacy of our predictive heterogeneity, we focus on the application of healthcare, utilizing the COVID-19 dataset of Brazilian patients. This dataset comprises 6882 COVID-positive patients from Brazil, whose data was recorded between February 27th and May 4th, 2020. The dataset includes a wide range of risk factors, including comorbidities, symptoms, and demographic characteristics. The binary label corresponds to mortality caused by COVID-19. Our aim is to validate the sub-populations learned through our methodology on this dataset, by thoroughly *explaining each group* and showcasing how our predictive heterogeneity can be employed to *uncover features related to mortality that are otherwise difficult to detect*.

5.2.1 LEARNED SUB-POPULATIONS.

When predicting mortality based on risk factors, it is important to consider that patients with various underlying diseases and demographic characteristics, such as age and sex, may exhibit different probabilities of mortality. Furthermore, it is plausible that the mortality of different individuals can be attributed to distinct factors. In light of these considerations, the predictive heterogeneity for this dataset is caused by the diversity of mechanisms that contribute to mortality among various sub-populations.

In this experiment, we use linear models and the loss function is binary cross-entropy loss. We select the sub-population number $K \in \{2, 3, 4, 5, 6\}$ that exhibit the maximal

empirical predictive heterogeneity $\hat{\mathcal{H}}_{\mathcal{V}}^{\mathcal{E}^K}(X \rightarrow Y; \mathcal{D})$, which results in three distinct subgroups (the optimal $K = 3$). Besides, we empirically observe that when $K > 3$, the learned sub-populations will shrink to 3 sub-populations. In Figure 5 and 6, to conduct a more thorough examination of the learned subgroups, we analyze the age distribution of each group, as well as the average value of their corresponding risk factors. Our analysis reveals several noteworthy findings:

1. We observe a distinct difference in the age distribution of the learned subgroups. Specifically, Group 0 is primarily composed of individuals over the age of 70, while Group 1 consists of individuals around 60 years old. Group 2, on the other hand, is comprised of middle-aged individuals spanning multiple age groups.
2. The average values of the risk factors reveal notable differences among the various subgroups, indicative of distinct causes of mortality. More specifically, Group 0 exhibits a considerably higher prevalence of underlying diseases, such as renal, neurologic, liver, and immunosuppression, when compared to the other groups. In contrast, Group 1 shows a substantially lower level of underlying diseases in comparison. Interestingly, Group 2 does not exhibit any underlying diseases, yet has a markedly higher level of diarrhea and vomiting. These findings suggest that the learned subgroups may be used to identify specific risk factors associated with mortality, which can inform targeted interventions for individuals with distinct risk profiles.

Having identified distinct patterns among the subgroups, we seek to identify the specific risk factors associated with mortality. To further validate our findings, we incorporate the expertise of domain experts. By leveraging their insights, we are able to confirm the reliability of the identified risk factors and the importance of our subgroup analysis.

5.2.2 SCIENTIFIC FINDINGS

Based on the learned group, we fit a logistic regression model on each group and pick the top-6 features with the largest coefficients, which are shown in Table 1.

Firstly, our analysis reveals that in Group 0 and 1, the top features associated with mortality are primarily SPO2 and underlying diseases, which align with the common risk factors of older individuals. In contrast, Group 2 exhibits a distinct set of top features, including symptoms of COVID-19 such as fever, cough, and vomiting. Notably, Group 2 is composed of middle-aged individuals spanning multiple age groups. Our findings suggest that severe COVID-19 symptoms can lead to mortality regardless of age.

Secondly, to further our analysis, we fit a model for the entire dataset and observe that the top features remain SPO2 and underlying diseases, consistent with the top features found for older individuals. However, this may not be beneficial or could even lead to harm for interventions targeted towards younger or middle-aged individuals who generally do not have severe underlying diseases. For instance, doctors may tend to treat younger patients with severe COVID-19 symptoms optimistically and underestimate their mortality risk because they typically do not have underlying diseases. Thus, exploring and leveraging the predictive heterogeneity within the data can lead to more reliable scientific discoveries while avoiding potential harm caused by latent heterogeneity.

Thirdly, our analysis reveals two important features in Group 2, namely vomiting and diarrhea, which are rarely considered in traditional analysis. We have reviewed relevant literature on COVID-19 and discovered that various studies have recognized these two symptoms as important indicators of higher risk of mortality caused by COVID-19. Zhong et al. (2020) highlighted the potential mechanisms of gastrointestinal and hepatic injuries in COVID-19 to raise awareness of digestive system injury in COVID-19. Liu et al. (2021b) analyzed 29,393 laboratory-confirmed COVID-19 patients diagnosed before March 21, 2020, in cities outside of Wuhan in mainland China and found that patients with both GI symptoms and fever and patients with fever alone had a significantly higher risk of death, where GI symptoms refer to one of the following symptoms: nausea, vomiting, diarrhea, or abdominal pain. Zeng et al. (2021) also found that gastrointestinal symptoms are associated with the severity of COVID-19, and the severe rate was more than 40% in COVID-19 patients with gastrointestinal symptoms. Ghimire et al. (2021) demonstrated that the presence of diarrhea as a presenting symptom is associated with increased disease severity and likely worse prognosis. Chan et al. (2022) have called for the consideration of COVID-19 in the differential diagnosis for patients who present with abdominal pain and gastrointestinal symptoms typical of gastroenteritis or surgical abdomen, even if they lack respiratory symptoms of COVID-19. These studies validate the reliability of our findings and demonstrate that studies utilizing the proposed predictive heterogeneity can uncover unusual risk factors that do not appear in analysis of the overall dataset.

This example serves as an illustration of the potential benefits that our predictive heterogeneity can offer to a wide range of scientific fields. By exploiting the heterogeneity within a dataset, our approach can reveal novel patterns and relationships that may be overlooked in traditional analyses, leading to more reliable and comprehensive scientific discoveries

Table 1: Top features of each learned subgroup and overall data on the COVID-19 dataset.

Group ID	Top Features					
0	SPO2	Diabetes	Renal	Neurologic	Pulmonary	Cardiovascular
1	Diabetes	SPO2	Neurologic	Cardiovascular	Pulmonary	Renal
2	Fever	Cough	Renal	Vomitting	Shortness of breath	Dihareea
All	SPO2	Renal	Neurologic	Diabetes	Pulmonary	Cardiovascular

5.3 Benefit Generalization

In this section, we aim to evaluate the efficacy of our IM algorithm in enhancing the out-of-distribution (OOD) generalization performance of machine learning models. To this end, we conduct experiments on both simulated data and real-world colored MNIST data. Our results suggest that the learned sub-population structures by our IM algorithm could significantly benefit the OOD generalization of machine learning models.

Baselines First, we compare with *empirical risk minimization* (ERM) and *environment inference for invariant learning* (EIL, (Creager et al., 2021)) which infers the environments for learning invariance. Then we compare with the well-known *KMeans* algorithm, which is the most popular clustering algorithm. For our IM algorithm and KMeans, we involve three algorithms as backbones to leverage the learned sub-populations, including sub-population balancing and invariant learning methods. The sub-population balancing

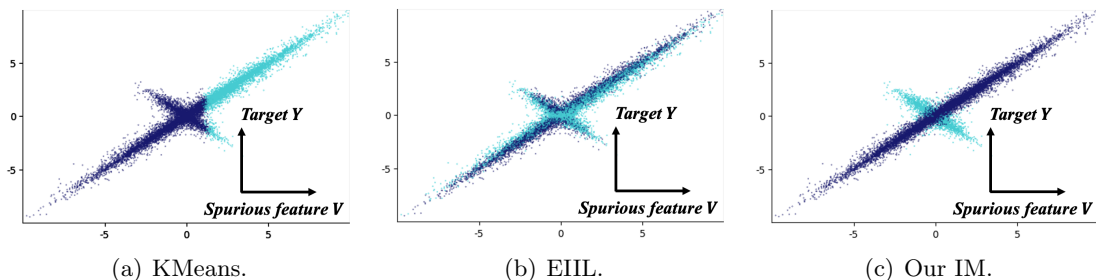


Figure 7: Sub-population division on the simulated data of three methods, where two colors denote two sub-populations.

simply equally weighs the learned sub-populations. *invariant risk minimization* (IRM, (Arjovsky et al., 2019)) and *inter-environment gradient alignment* (IGA, (Koyama and Yamaguchi, 2020)) are typical methods in OOD generalization, which take the sub-populations as input environments to learn the invariant models.

5.3.1 SIMULATION DATA OF SAMPLE SELECTION BIAS

The input features $X = [S, T, V]^T \in \mathbb{R}^{10}$ consist of stable features $S \in \mathbb{R}^5$, noisy features $T \in \mathbb{R}^4$ and the spurious feature $V \in \mathbb{R}$:

$$S \sim \mathcal{N}(0, 2\mathbf{I}_5), T \sim \mathcal{N}(0, 2\mathbf{I}_4), Y = \theta_S^T S + h(S) + \mathcal{N}(0, 0.5), V \sim \text{Laplace}(\text{sign}(r) \cdot Y, 1/(5 \ln |r|)) \quad (41)$$

where $\theta_S \in \mathbb{R}^5$ is the coefficient and $h(S) = S_1 S_2 S_3$ is the nonlinear term. $|r| > 1$ is a factor for each sub-population, and here the data heterogeneity is brought by the *endogeneity with hidden variable* (Fan et al., 2014). V is the *spurious feature* whose relationship with Y is unstable across sub-populations and is controlled by the factor r . Intuitively, $\text{sign}(r)$ controls whether the spurious correlation between V and Y is positive or negative. And $|r|$ controls the strength of the spurious correlation, i.e. the larger $|r|$ means the stronger spurious correlation. In *training*, we generate 10000 points, where the major group contains 80% data with $r = 1.9$ (i.e. strong *positive* spurious correlation) and the minor group contains 20% data with $r = -1.9$ (i.e. strong *negative* spurious correlation). In *testing*, we test the performances of the two groups respectively, and we also set $r = -2.3$ and $r = -2.7$

Table 2: Results of the experiments on out-of-distribution generalization, including the simulated data and colored MNIST data.

Method	1. Simulated Data				2. Colored MNIST		
	Training Sub-population Error		Test Error		Train Accuracy	Test Accuracy	
	Major ($r = 1.9$)	Minor ($r = -1.9$)	$r = -2.3$	$r = -2.7$			
ERM	0.255(± 0.024)	0.740(± 0.022)	0.738(± 0.035)	0.737(± 0.023)	0.998(± 0.001)	0.406(± 0.019)	
EILL	0.164 (± 0.014)	1.428(± 0.035)	1.431(± 0.061)	1.431(± 0.046)	0.812(± 0.006)	0.610(± 0.016)	
KMeans	Balance	0.231(± 0.022)	0.847(± 0.024)	0.846(± 0.039)	0.845(± 0.026)	0.999 (± 0.001)	0.328(± 0.021)
	IRM	0.231(± 0.022)	0.845(± 0.024)	0.844(± 0.039)	0.843(± 0.026)	0.947(± 0.004)	0.259(± 0.021)
Ours	IGA	0.235(± 0.022)	0.840(± 0.023)	0.839(± 0.038)	0.838(± 0.027)	0.997(± 0.001)	0.302(± 0.021)
	Balance	0.403(± 0.041)	0.423 (± 0.016)	0.416 (± 0.022)	0.416 (± 0.014)	0.749(± 0.012)	0.692 (± 0.039)
	IRM	0.391(± 0.039)	0.432 (± 0.016)	0.430 (± 0.022)	0.430 (± 0.014)	0.759(± 0.014)	0.727 (± 0.047)
	IGA	0.449(± 0.037)	0.426 (± 0.017)	0.417 (± 0.022)	0.417 (± 0.014)	0.759(± 0.012)	0.713 (± 0.034)

to simulate stronger distributional shifts. We use linear regression and set $K = 2$ for all methods, and we report the mean-square errors (MSE) of all methods.

The results over 10 runs are shown in Table 2. From the results in Table 2, for both the simulated and colored MNIST data, the two backbones with our IM algorithm achieve *the best OOD generalization performances*. Also, for the simulated data, the learned predictive heterogeneity enables backbone algorithms to equally treat the majority and minority inside data (i.e. low-performance gap between 'Major' and 'Minor'), and significantly benefits the OOD generalization. Further, we plot the learned sub-populations of our IM algorithm in Figure 7. From Figure 7, compared with KMeans and EIIL, our predictive heterogeneity exploits the spurious correlation between V and Y , and enables the backbone algorithms to eliminate it.

5.3.2 SIMULATION DATA OF HIDDEN VARIABLES

Also, we add one more experiment to show that (1) when the chosen K is smaller than the ground-truth, the performances of our methods will drop but are still better than ERM (2) when the chosen K is larger, the performances are not affected much.

The input features $X = [S, T, V] \in \mathbb{R}^{10}$ consist of stable features $S \in \mathbb{R}^5$, noisy features $T \in \mathbb{R}^4$ and the spurious feature $V \in \mathbb{R}$:

$$S \sim \mathcal{N}(2, 2\mathbb{I}_5), \quad T \sim \mathcal{N}(0, 2\mathbb{I}_4), \quad Y = \theta_S^T S + S_1 S_2 S_3 + \mathcal{N}(0, 0.5),$$

and we generate the spurious feature via:

$$V = \theta_V^e Y + \mathcal{N}(0, 0.3),$$

where θ_V^e varies across sub-populations and is dependent on which sub-population the data point belongs to. In training, we sample 8000 data points from e_1 with $\theta_V^1 = 3.0$, 1000 points from e_2 with $\theta_V^2 = -1.0$, 1000 points from e_3 with $\theta_V^3 = -2.0$ and 1000 points from e_4 with $\theta_V^4 = -3.0$. Therefore, the ground-truth number of sub-populations is 4. In testing, we test the performances on e_4 with $\theta_V^4 = -3.0$, which has strong distributional shifts from training data. The average MSE over 10 runs are shown in Figure 8.

From the results, we can see that when K is smaller than the ground-truth, increasing K benefits the OOD generalization performance, and when K is larger, the performances are not affected much.

For our IM algorithm, we think there are mainly two ways to choose K :

- According to the predictive heterogeneity index: When the chosen K is smaller than the ground-truth, our measure tends to increase quickly when increasing K ; and when K is larger than the ground-truth, the increasing speed will slow down, which could direct people to choose an appropriate K .
- According to the prediction model: Since our IM algorithm aims to learn sub-populations with different prediction mechanisms, one could compare the learned model parameters $\theta_1, \dots, \theta_K$ to judge whether K is much larger than the ground-truth, i.e., if two resultant models are quite similar, K may be too large (divide one sub-population into two). For linear models, one can directly compare the coefficients. For deep models, we think one can calculate the transfer losses across sub-populations.

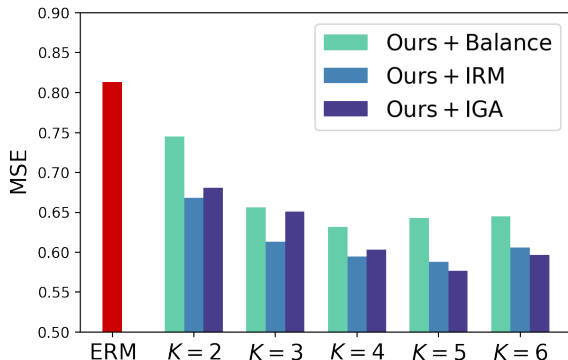


Figure 8: The OOD generalization error of our methods with Sub-population Balancing, IRM and IGA as backbones for the added experiments. The ground-truth sub-population number is 4.

5.3.3 COLORED MNIST

Following Arjovsky et al. (2019), we design a binary classification task constructed on the MNIST dataset. Firstly, digits 0 ~ 4 are labeled $Y = 0$ and digits 5 ~ 9 are labeled $Y = 1$. Secondly, noisy labels \tilde{Y} are induced by randomly flipping the label Y with a probability of 0.2. Then we sample the colored id V spurious correlated with \tilde{Y} as

$$V = \begin{cases} +\tilde{Y}, & \text{with probability } r, \\ -\tilde{Y}, & \text{with probability } 1 - r. \end{cases} \quad (42)$$

In fact, r controls the spurious correlation between \tilde{Y} and V . In *training*, we randomly sample 10000 data points and set $r = 0.85$, meaning that for 85% of the data, V is positively correlated with \tilde{Y} and for the rest 15%, the spurious correlation becomes negative, which causes data heterogeneity w.r.t. V and \tilde{Y} . In *testing*, we set $r = 0$ (*strong negative spurious correlation*), bringing strong shifts between training and testing.

From the results in Table 2, for both the simulated and colored MNIST data, the two backbones with our IM algorithm achieve *the best OOD generalization performances*. We plot the learned sub-populations of our IM algorithm in Figure 9. From Figure 9, the learned sub-populations of our method also reflect the different directions of the spurious correlation between digit labels Y and colors (red or green), which helps backbone methods to avoid using colors to predict digits.

6 Related Work

To the best of our knowledge, data heterogeneity has not converged to a uniform formulation so far, and has different meanings among different fields. Li and Reynolds (1995) define the heterogeneity in *ecology* based on the system property and complexity or variability. Rosenbaum (2005) views the uncertainty of the potential outcome as unit heterogeneity in observational studies in *economics*. For *graph* data, the heterogeneity refers to various types of nodes and edges (Wang et al. (2019)). More recently, in machine learning, several



Figure 9: Sub-population division on the MNIST data of our IM algorithm.

works of *causal learning* (Peters et al., 2016; Arjovsky et al., 2019; Koyama and Yamaguchi, 2020; Creager et al., 2021) and *robust learning* (Sagawa et al., 2019) leverage heterogeneous data from multiple environments to improve the out-of-distribution generalization ability. Specifically, invariant learning methods (Arjovsky et al., 2019; Koyama and Yamaguchi, 2020; Creager et al., 2021; Zhou et al., 2022) leverage the heterogeneous environment to learn the invariant predictors that have uniform performances across environments. And in distributionally robust optimization field, Sagawa et al. (2019); Duchi et al. (2022) propose to optimize the worst-group prediction error to guarantee the OOD generalization performance. However, in machine learning, previous works have not provided a precise definition or sound quantification of data heterogeneity, which makes it confusing and hard to leverage to develop more rational machine learning algorithms.

As for clustering algorithms, most algorithms only focus on the covariates X , typified by KMeans and Gaussian Mixture Model (GMM, (Reynolds, 2009)). However, the learned clusters by KMeans can only reflect heterogeneous structures in $P(X)$, which is shown by our experiments. Notably that our predictive heterogeneity could reflect the heterogeneity in $P(Y|X)$. And the expectation maximization (EM, (Moon, 1996)) can also be used for clustering. However, our IM algorithm has essential differences from EM, for our IM algorithm infers latent variables that maximizes the predictive heterogeneity but EM maximizes the likelihood. Also, there are methods (Creager et al., 2021) from the invariant learning field to infer environments. Though it could benefit the OOD generalization, it lacks the theoretical foundation and only works in some settings.

7 Discussion on differences with sub-group discovery

Subgroup discovery (SD, (Helal, 2016)) is aimed at extracting "interesting" relations among different variables (X) with respect to a target variable Y . Coverage and precision of each discovered group is the focus of such method. To be specific, it learns a partition on $P(X)$ such that some target label y dominates within each group. The most significant gap between subgroup discovery and our predictive heterogeneity lies in the pattern of distributional shift among clusters: for subgroup discovery, $P(X)$ and $P(Y)$ varies across subgroups but there is a universal $P(Y|X)$. While for predictive heterogeneity $P(Y|X)$ differs across sub-population, which indicates diversified prediction mechanism. It is such disparity of prediction mechanism that inhibits the performance of a universal predictive model on a heterogeneous dataset, which is the emphasis of OOD problem and group fairness.

We think sub-group discovery is more applicable for settings where the distributional shift is minor while high explainability is required, since it generates simplified rules that people can understand. Also, sub-group discovery methods is suitable for the settings that only involve tabular data (typically from a relational database), where the input features have clear semantics. And our proposed method could deal with general machine learning settings, including complicated data (e.g., image data) that involves representation learning. Also, when people have to handle settings where data heterogeneity w.r.t. prediction mechanism exists inside data, our method is more applicable. However, both kinds of methods can be used to help people understand data and make more reasonable decisions.

8 Discussion on the Potential for fairness

We find combining our measure with algorithmic fairness is an interesting and promising direction and we think our measure has the potential to deal with algorithmic bias. Our method could generate sub-populations with possibly different prediction mechanisms, which could do some help in the following aspects:

Risk feature selection: we could select features according to our predictive heterogeneity measure to see what features bring the largest heterogeneity. If they are sensitive features, people should avoid their effects, and if they are not, they could direct people to build better machine learning models.

Examine the algorithmic fairness: we could use the learned sub-populations to examine whether a given algorithm is fair by calculating the performance gap across the sub-populations.

9 Conclusion

We define the predictive heterogeneity, as the first quantitative formulation of the data heterogeneity that affects the prediction of machine learning models. We demonstrate its theoretical properties and show that it benefits the out-of-distribution generalization performances.

Appendix A. Proof of Proposition 6

Proof [Proof of Proposition 6]

1. *Monotonicity:*

Because of $\mathcal{E}_1 \subseteq \mathcal{E}_2$,

$$\mathcal{H}_{\mathcal{V}}^{\mathcal{E}_1}(X \rightarrow Y) = \sup_{\mathcal{E} \in \mathcal{E}_1} \mathbb{I}_{\mathcal{V}}(X \rightarrow Y|\mathcal{E}) - \mathbb{I}_{\mathcal{V}}(X \rightarrow Y) \quad (43)$$

$$\leq \sup_{\mathcal{E} \in \mathcal{E}_2} \mathbb{I}_{\mathcal{V}}(X \rightarrow Y|\mathcal{E}) - \mathbb{I}_{\mathcal{V}}(X \rightarrow Y) \quad (44)$$

$$= \mathcal{H}_{\mathcal{V}}^{\mathcal{E}_2}(X \rightarrow Y). \quad (45)$$

2. *Nonnegativity:*

According to the definition of the environment set, there exists $\mathcal{E}_0 \in \mathcal{E}$ such that for any $e \in \text{supp}(\mathcal{E})$, $X, Y|\mathcal{E} = e$ is identically distributed as X, Y . Thus, we have

$$\mathcal{H}_{\mathcal{V}}^{\mathcal{E}}(X \rightarrow Y) = \sup_{\mathcal{E} \in \mathcal{E}} [H_{\mathcal{V}}(Y|\emptyset, \mathcal{E}) - H_{\mathcal{V}}(Y|X, \mathcal{E})] - [H_{\mathcal{V}}(Y|\emptyset) - H_{\mathcal{V}}(Y|X)] \quad (46)$$

$$\geq [H_{\mathcal{V}}(Y|\emptyset, \mathcal{E}_0) - H_{\mathcal{V}}(Y|X, \mathcal{E}_0)] - [H_{\mathcal{V}}(Y|\emptyset) - H_{\mathcal{V}}(Y|X)]. \quad (47)$$

Specifically,

$$H_{\mathcal{V}}(Y|X, \mathcal{E}_0) = \mathbb{E}_{e \sim \mathcal{E}_0} \left[\inf_{f \in \mathcal{V}} \mathbb{E}_{x, y \sim X, Y|\mathcal{E}=e} [-\log f[x](y)] \right] \quad (48)$$

$$= \mathbb{E}_{e \sim \mathcal{E}_0} \left[\inf_{f \in \mathcal{V}} \mathbb{E}_{x, y \sim X, Y} [-\log f[x](y)] \right] \quad (49)$$

$$= H_{\mathcal{V}}(Y|X). \quad (50)$$

Similarly, $H_{\mathcal{V}}(Y|\emptyset, \mathcal{E}_0) = H_{\mathcal{V}}(Y|\emptyset)$. Thus, $\mathcal{H}_{\mathcal{V}}^{\mathcal{E}}(X \rightarrow Y) \geq 0$.

3. *Boundedness:*

First, we have

$$H_{\mathcal{V}}(Y|X, \mathcal{E}) = \mathbb{E}_{e \sim \mathcal{E}} \left[\inf_{f \in \mathcal{V}} \mathbb{E}_{x, y \sim X, Y|\mathcal{E}=e} [-\log f[x](y)] \right] \quad (51)$$

$$= \mathbb{E}_{e \sim \mathcal{E}} \left[\inf_{f \in \mathcal{V}} \mathbb{E}_{x \sim X|\mathcal{E}=e} [\mathbb{E}_{y \sim Y|x, e} [-\log f[x](y)]] \right] \quad (52)$$

$$\geq 0, \quad (53)$$

by noticing that $\mathbb{E}_{y \sim Y|x} [-\log f[x](y)]$ is the cross entropy between $Y|x, e$ and $f[x]$.

Next,

$$H_{\mathcal{V}}(Y|\emptyset, \mathcal{E}) = \mathbb{E}_{e \sim \mathcal{E}} \left[\inf_{f \in \mathcal{V}} \mathbb{E}_{y \sim Y|\mathcal{E}=e} [-\log f[\emptyset](y)] \right] \quad (54)$$

$$\leq \inf_{f \in \mathcal{V}} \mathbb{E}_{e \sim \mathcal{E}} [\mathbb{E}_{y \sim Y|\mathcal{E}=e} [-\log f[\emptyset](y)]] \quad (55)$$

$$= \inf_{f \in \mathcal{V}} \mathbb{E}_{y \sim Y} [-\log f[\emptyset](y)] \quad (56)$$

$$= H_{\mathcal{V}}(Y|\emptyset), \quad (57)$$

where Equation 55 is due to Jensen's inequality.

Combing the above inequalities,

$$\mathcal{H}_V^\mathcal{E}(X \rightarrow Y) = \sup_{\mathcal{E} \in \mathcal{E}} [H_V(Y|\emptyset, \mathcal{E}) - H_V(Y|X, \mathcal{E})] - [H_V(Y|\emptyset) - H_V(Y|X)] \quad (58)$$

$$\leq \sup_{\mathcal{E} \in \mathcal{E}} H_V(Y|\emptyset, \mathcal{E}) - [H_V(Y|\emptyset) - H_V(Y|X)] \quad (59)$$

$$\leq H_V(Y|\emptyset) - [H_V(Y|\emptyset) - H_V(Y|X)] \quad (60)$$

$$= H_V(Y|X). \quad (61)$$

4. Corner Case:

According to Proposition 2 in Xu et al. (2020),

$$H_\Omega(Y|\emptyset) = H(Y). \quad (62)$$

$$H_\Omega(Y|X) = H(Y|X). \quad (63)$$

By taking random variables R, S identically distributed as $X, Y|\mathcal{E} = e$ for $e \in \text{supp}(\mathcal{E})$, we have

$$H_\Omega(Y|X, \mathcal{E} = e) = H_\Omega(S|R) = H(S|R) = H(Y|X, \mathcal{E} = e). \quad (64)$$

Thus,

$$H_\Omega(Y|X, \mathcal{E}) = \mathbb{E}_{e \sim \mathcal{E}} [H_\Omega(Y|X, \mathcal{E} = e)] = \mathbb{E}_{e \sim \mathcal{E}} [H(Y|X, \mathcal{E} = e)] = H(Y|X, \mathcal{E}). \quad (65)$$

Similarly, we have $H_\Omega(Y|\emptyset, \mathcal{E}) = H(Y|\mathcal{E})$. Thus,

$$\mathcal{H}_\Omega^\mathcal{E}(X \rightarrow Y) = \sup_{\mathcal{E} \in \mathcal{E}} [H_\Omega(Y|\emptyset, \mathcal{E}) - H_\Omega(Y|X, \mathcal{E})] - [H_\Omega(Y|\emptyset) - H_\Omega(Y|X)] \quad (66)$$

$$= \sup_{\mathcal{E} \in \mathcal{E}} [H(Y|\mathcal{E}) - H(Y|X, \mathcal{E})] - [H(Y) - H(Y|X)] \quad (67)$$

$$= \sup_{\mathcal{E} \in \mathcal{E}} \mathbb{I}(Y; X|\mathcal{E}) - \mathbb{I}(Y; X) \quad (68)$$

$$= \mathcal{H}^\mathcal{E}(X, Y). \quad (69)$$

■

Appendix B. Proof of Theorem 7

Proof [Proof of Theorem 7]

1)

$$H_{\mathcal{V}_G}(Y|X) = \inf_{f \in \mathcal{V}_G} \mathbb{E}_{x \sim X} [\mathbb{E}_{y \sim Y|x} [-\log f[x](y)]] \quad (70)$$

$$\leq \mathbb{E}_{x \sim X} \left[\mathbb{E}_{y \sim Y|x} \left[-\log \frac{1}{\sqrt{2\pi} \cdot \frac{1}{\sqrt{2\pi}}} \exp \left[-\frac{(y - g(x))^2}{2 \cdot \frac{1}{2\pi}} \right] \right] \right] \quad (71)$$

$$= \mathbb{E}_{x \sim X} [\mathbb{E}_{y \sim Y|x} [\pi(y - g(x))^2]] = \pi\sigma^2. \quad (72)$$

Equation 71 holds by taking $f[x] = \mathcal{N}(g(x), \frac{1}{2\pi})$.

2)

Given the function family $\mathcal{V}_\sigma = \{f|f[x] = \mathcal{N}(\theta x, \sigma^2), \theta \in \mathbb{R}, \sigma \text{ fixed}\}$, by expanding the Gaussian probability density function in the definition of predictive \mathcal{V} -information, it could be shown that

$$\mathbb{I}_{\mathcal{V}_\sigma}(X \rightarrow Y) \propto \min_{k \in \mathbb{R}} -\mathbb{E}[(Y - kX)^2] + \text{Var}(Y), \quad (73)$$

where the predictive \mathcal{V} -information is proportional to Mean Square Error subtracted by the variance of target, by a coefficient completely dependent on σ .

The minimization problem is solved by

$$k = \frac{\mathbb{E}[XY]}{\mathbb{E}[X^2]} = 1. \quad (74)$$

Substituting k into eq.73,

$$\mathbb{I}_{\mathcal{V}_\sigma}(X \rightarrow Y) \propto (-\mathbb{E}[\epsilon^2] + \text{Var}(X + \epsilon)) = \text{Var}(X) = \mathbb{E}[X^2]. \quad (75)$$

Denote $\text{supp}(\mathcal{E}) = \{\mathcal{E}_1, \mathcal{E}_2\}$. Let Q be the joint distribution of $(X, \epsilon, \mathcal{E})$. Let $Q(\mathcal{E}_1) = \alpha$ and $Q(\mathcal{E}_2) = 1 - \alpha$ be the marginal of \mathcal{E} . Abbreviate $Q(X, \epsilon | \mathcal{E} = \mathcal{E}_1)$ by $P_1(X, \epsilon)$ and $Q(X, \epsilon | \mathcal{E} = \mathcal{E}_2)$ by $P_2(X, \epsilon)$.

Similar to 73,

$$\mathbb{I}_{\mathcal{V}_\sigma}(X \rightarrow Y | \mathcal{E}) \propto \min_k -\mathbb{E}[(Y - kX)^2 | \mathcal{E}] + \text{Var}(Y | \mathcal{E}). \quad (76)$$

For $\mathcal{E} = \mathcal{E}_1$, the minimization problem is solved by

$$k = \frac{\mathbb{E}_{P_1}[XY]}{\mathbb{E}_{P_1}[X^2]}. \quad (77)$$

Thus,

$$\mathbb{I}_{\mathcal{V}_\sigma}(X \rightarrow Y | \mathcal{E} = \mathcal{E}_1) \propto -\mathbb{E}_{P_1} \left[\left(Y - \frac{\mathbb{E}_{P_1}[XY]}{\mathbb{E}_{P_1}[X^2]} X \right)^2 \right] + \text{Var}_{P_1}(Y) \quad (78)$$

$$= -\mathbb{E}_{P_1}[Y^2] + \frac{\mathbb{E}_{P_1}^2[XY]}{\mathbb{E}_{P_1}[X^2]} + (\mathbb{E}_{P_1}[Y^2] - \mathbb{E}_{P_1}^2[Y]) = -\mathbb{E}_{P_1}^2[Y] + \frac{\mathbb{E}_{P_1}^2[XY]}{\mathbb{E}_{P_1}[X^2]}. \quad (79)$$

Similarly, we have

$$\mathbb{I}_{\mathcal{V}_\sigma}(X \rightarrow Y | \mathcal{E} = \mathcal{E}_2) \propto -\mathbb{E}_{P_2}^2[Y] + \frac{\mathbb{E}_{P_2}^2[XY]}{\mathbb{E}_{P_2}[X^2]}. \quad (80)$$

Notably, $\mathbb{E}_{P_1}[X^2]$ and $\mathbb{E}_{P_2}[X^2]$ are constrained by α and $\mathbb{E}[X^2]$.

$$\mathbb{E}[X^2] = \mathbb{E}[\mathbb{E}[X^2 | \mathcal{E}]] = \alpha \mathbb{E}_{P_1}[X^2] + (1 - \alpha) \mathbb{E}_{P_2}[X^2]. \quad (81)$$

Similarly,

$$\mathbb{E}[XY] = \mathbb{E}[XY] = \alpha \mathbb{E}_{P_1}[XY] + (1 - \alpha) \mathbb{E}_{P_2}[XY]. \quad (82)$$

$$0 = \mathbb{E}[Y] = \alpha \mathbb{E}_{P_1}[Y] + (1 - \alpha) \mathbb{E}_{P_2}[Y]. \quad (83)$$

The moments of P_2 could thereafter be represented by those of P_1 .

$$\mathbb{E}_{P_2}[X^2] = \frac{\mathbb{E}[X^2] - \alpha \mathbb{E}_{P_1}[X^2]}{1 - \alpha}, \mathbb{E}_{P_2}[XY] = \frac{\mathbb{E}[X^2] - \alpha \mathbb{E}_{P_1}[XY]}{1 - \alpha}, \mathbb{E}_{P_2}[Y] = -\frac{\alpha \mathbb{E}_{P_1}[Y]}{1 - \alpha}. \quad (84)$$

Substituting to eq.80,

$$\mathbb{I}_{\mathcal{V}_\sigma}(X \rightarrow Y | \mathcal{E} = \mathcal{E}_2) \propto -\frac{\alpha^2}{(1 - \alpha)^2} E_{P_1}^2[Y] + \frac{1}{1 - \alpha} \frac{(\mathbb{E}[X^2] - \alpha \mathbb{E}_{P_1}[XY])^2}{\mathbb{E}[X^2] - \alpha \mathbb{E}_{P_1}[X^2]}. \quad (85)$$

Thus,

$$\mathcal{H}_{\mathcal{V}_\sigma}^\mathcal{E}(X \rightarrow Y) = \sup_{\mathcal{E} \in \mathcal{E}} -\mathbb{I}_{\mathcal{V}_\sigma}(X \rightarrow Y) + \alpha \mathbb{I}_{\mathcal{V}_\sigma}(X \rightarrow Y | \mathcal{E} = \mathcal{E}_1) + (1 - \alpha) \mathbb{I}_{\mathcal{V}_\sigma}(X \rightarrow Y | \mathcal{E} = \mathcal{E}_2) \quad (86)$$

$$\propto \sup_{\mathcal{E} \in \mathcal{E}} -\mathbb{E}[X^2] - \alpha \mathbb{E}_{P_1}^2[Y] + \alpha \frac{\mathbb{E}_{P_1}^2[XY]}{\mathbb{E}_{P_1}[X^2]} - \frac{\alpha^2}{1 - \alpha} \mathbb{E}_{P_1}^2[Y] + \frac{(\mathbb{E}[X^2] - \alpha \mathbb{E}_{P_1}[XY])^2}{\mathbb{E}[X^2] - \alpha \mathbb{E}_{P_1}[X^2]} \quad (87)$$

$$= \sup_{\mathcal{E} \in \mathcal{E}} -\frac{\alpha}{1 - \alpha} \mathbb{E}_{P_1}^2[X + \epsilon] + \alpha \frac{\mathbb{E}_{P_1}^2[X\epsilon]}{\mathbb{E}_{P_1}[X^2] (\mathbb{E}[X^2] - \alpha \mathbb{E}_{P_1}[X^2])} \mathbb{E}[X^2]. \quad (88)$$

Assuming $X \perp \epsilon | \mathcal{E}$,

$$\mathcal{H}_{\mathcal{V}_\sigma}^\mathcal{E}(X \rightarrow Y) \propto \sup_{\mathcal{E} \in \mathcal{E}} -\frac{\alpha}{1 - \alpha} \mathbb{E}_{P_1}^2[X + \epsilon] \leq 0. \quad (89)$$

From Proposition 6, we have $\mathcal{H}_{\mathcal{V}_\sigma}^\mathcal{E}(X \rightarrow Y) \geq 0$. Thus, $\mathcal{H}_{\mathcal{V}_\sigma}^\mathcal{E}(X \rightarrow Y) = 0$. ■

Appendix C. Proof of Linear Cases (Theorem 8 and 9)

Proof [Proof of Theorem 8]

For the ease of notion, we denote the $r(\mathcal{E}^*)$ as r_e , $\sigma(\mathcal{E}^*)$ as σ_e , and $\sigma(\mathcal{E}^*) \cdot \epsilon_v$ as ϵ_e . And we omit the superscript \mathcal{C} of $\mathcal{H}_{\mathcal{V}}$. Firstly, we calculate the $H_{\mathcal{V}}[Y|\emptyset]$ as:

$$H_{\mathcal{V}}[Y|\emptyset] = \frac{1}{2\sigma^2} \text{Var}(Y) + \log \sigma + \frac{1}{2} \log 2\pi, \quad (90)$$

$$H_{\mathcal{V}}[Y|\emptyset, \mathcal{E}^*] = \frac{1}{2\sigma^2} \mathbb{E}_{\mathcal{E}^*}[\text{Var}(Y|\mathcal{E}^*)] + \log \sigma + \frac{1}{2} \log 2\pi. \quad (91)$$

Therefore, we have

$$H_{\mathcal{V}}[Y|\emptyset, \mathcal{E}^*] - H_{\mathcal{V}}[Y|\emptyset] = -\frac{1}{2\sigma^2} \text{Var}(\mathbb{E}[Y|\mathcal{E}^*]) \leq 0. \quad (92)$$

As for $H_{\mathcal{V}}[Y|X]$, we have

$$H_{\mathcal{V}}[Y|X] = \inf_{h_S, h_V} \mathbb{E}_{X,Y} [\|Y - (h_S S + h_V V)\|^2] \frac{1}{2\sigma^2} \quad (93)$$

$$= \inf_{h_S, h_V} \mathbb{E}_{\mathcal{E}^*} [\mathbb{E}[\|f(S) + \epsilon_Y - (h_S S + h_V(r_e f(S) + \epsilon_e))\|^2 | \mathcal{E}^*]] \frac{1}{2\sigma^2}, \quad (94)$$

where we let $h_S = h_S - \beta$ here. Then we have

$$2\sigma^2 H_V[Y|X] = \inf_{h_S, h_V} \mathbb{E}_{\mathcal{E}^*} [\mathbb{E}[\|(1 - h_V r_e)f(S) + \epsilon_Y - h_S S - h_V \epsilon_e\|^2 | \mathcal{E}^*]] \quad (95)$$

$$= \inf_{h_S, h_V} \mathbb{E}_{\mathcal{E}^*} [\mathbb{E}[\|(1 - h_V r_e)f(S) - h_S S\|^2 | \mathcal{E}^*]] + \sigma_Y^2 + h_V^2 \mathbb{E}_{\mathcal{E}^*}[\sigma_e^2], \quad (96)$$

notably that here for $e_i, e_j \in \text{supp}(\mathcal{E}^*)$, we assume $P^{e_i}(S, Y) = P^{e_j}(S, Y)$ (we choose such \mathcal{E}^* as one possible split). And the solution of h_S, h_V is

$$h_S = \frac{\text{Var}(r_e) \mathbb{E}[f^2(S)] \mathbb{E}[f(S)S] + \mathbb{E}[\sigma_e^2] \mathbb{E}[f(S)S]}{\mathbb{E}[r_e^2] \mathbb{E}[f^2(S)] \mathbb{E}[S^2] + \mathbb{E}[\sigma_e^2] \mathbb{E}[S^2] - \mathbb{E}^2[r_e] \mathbb{E}^2[f(S)S]}, \quad (97)$$

$$h_V = \frac{\mathbb{E}[r_e] (\mathbb{E}[f^2(S)] \mathbb{E}[S^2] - \mathbb{E}^2[f(S)S])}{\mathbb{E}[r_e^2] \mathbb{E}[f^2(S)] \mathbb{E}[S^2] + \mathbb{E}[\sigma_e^2] \mathbb{E}[S^2] - \mathbb{E}^2[r_e] \mathbb{E}^2[f(S)S]}. \quad (98)$$

According to the assumption that $\mathbb{E}[f(S)S] = 0$, we have

$$h_S = 0, \quad h_V = \frac{\mathbb{E}[r(\mathcal{E}^*)] \mathbb{E}[f^2]}{\mathbb{E}[r^2(\mathcal{E}^*)] \mathbb{E}[f^2] + \mathbb{E}[\sigma^2(\mathcal{E}^*)]}. \quad (99)$$

Therefore, we have

$$2\sigma^2 H_V[Y|X] = \mathbb{E}_{\mathcal{E}^*} [\mathbb{E}[\|(1 - h_V r_e)f(S)\|^2 | \mathcal{E}^*]] + \sigma_Y^2 + h_V^2 \mathbb{E}_{\mathcal{E}^*}[\sigma_e^2] \quad (100)$$

$$= \frac{\text{Var}(r_e) \mathbb{E}[f^2] + \mathbb{E}[\sigma^2(\mathcal{E}^*)]}{\mathbb{E}[r_e^2] \mathbb{E}[f^2] + \mathbb{E}[\sigma^2(\mathcal{E}^*)]} \mathbb{E}[f^2(S)] + \sigma_Y^2, \quad (101)$$

$$2\sigma^2 H_V[Y|X, \mathcal{E}^*] = \sigma_Y^2 + \mathbb{E}[(\frac{1}{\frac{r_e^2 \mathbb{E}[f^2]}{\sigma_e^2} + 1})^2] \mathbb{E}[f^2] + \mathbb{E}_{\mathcal{E}^*}[(\frac{1}{\frac{r_e}{\sigma_e} + \frac{\sigma_e}{r_e \mathbb{E}[f^2]}})^2]. \quad (102)$$

Note that here we simply set $\sigma = 1$ in the main body. And we have:

$$\mathcal{H}_V(X \rightarrow Y) \approx \frac{\text{Var}(r_e) \mathbb{E}[f^2] + \mathbb{E}[\sigma^2(\mathcal{E}^*)]}{\mathbb{E}[r_e^2] \mathbb{E}[f^2] + \mathbb{E}[\sigma^2(\mathcal{E}^*)]} \mathbb{E}[f^2(S)] \quad (103)$$

The approximation error is bounded by $\frac{1}{2} \max(\sigma_Y^2, R(r(\mathcal{E}^*), \sigma(\mathcal{E}^*), \mathbb{E}[f^2]))$, and $R(r(\mathcal{E}^*), \sigma(\mathcal{E}^*), \mathbb{E}[f^2])$ is defined as:

$$R(r(\mathcal{E}^*), \sigma(\mathcal{E}^*), \mathbb{E}[f^2]) = \mathbb{E}[(\frac{1}{\frac{r_e^2 \mathbb{E}[f^2]}{\sigma_e^2} + 1})^2] \mathbb{E}[f^2] + \mathbb{E}_{\mathcal{E}^*}[(\frac{1}{\frac{r_e}{\sigma_e} + \frac{\sigma_e}{r_e \mathbb{E}[f^2]}})^2] \quad (104)$$

■

Proof [Proof of Theorem 9] Similar as the above proof. ■

Appendix D. Proof of the Error Bound for Finite Sample Estimation (Theorem 11)

In this section, we will prove the error bound of estimating the predictive heterogeneity with the empirical predictive heterogeneity. Before the proof of Theorem 11 which is inspired by Xu et al. (2020), we will introduce three lemmas.

Lemma 14 *Assume $\forall x \in \mathcal{X}, \forall y \in \mathcal{Y}, \forall f \in \mathcal{V}, \log f[x](y) \in [-B, B]$ where $B > 0$. Define a function class $\mathcal{G}_{\mathcal{V}}^k = \{g | g(x, y) = \log f[x](y)q(\mathcal{E} = e_k | x, y), f \in \mathcal{V}, q \in \mathcal{Q}\}$. Denote the Rademacher complexity of \mathcal{G} with N samples by $\mathcal{R}_N(\mathcal{G})$. Define*

$$\hat{f}_k = \arg \inf_f \frac{1}{|\mathcal{D}|} \sum_{x_i, y_i \in \mathcal{D}} -\log f[x_i](y_i)q(\mathcal{E} = e_k | x_i, y_i). \quad (105)$$

Then for any $q \in \mathcal{Q}$, any $\delta \in (0, 1)$, with a probability over $1 - \delta$, we have

$$\left| q(\mathcal{E} = e_k)H_{\mathcal{V}}(Y|X, \mathcal{E} = e_k) - \frac{1}{|\mathcal{D}|} \sum_{x_i, y_i \in \mathcal{D}} -\log \hat{f}_k[x_i](y_i)q(\mathcal{E} = e_k | x_i, y_i) \right| \quad (106)$$

$$\leq 2\mathcal{R}_{|\mathcal{D}|}(\mathcal{G}_{\mathcal{V}}^k) + B\sqrt{\frac{2 \log \frac{1}{\delta}}{|\mathcal{D}|}}. \quad (107)$$

Proof Apply McDiarmid's inequality to the function $\Phi(\mathcal{D})$ which is defined as:

$$\Phi(\mathcal{D}) = \sup_{f \in \mathcal{V}, q \in \mathcal{Q}} \left| q(\mathcal{E} = e_k)\mathbb{E}_q[-\log f[x](y)|\mathcal{E} = e_k] - \frac{1}{|\mathcal{D}|} \sum_{x_i, y_i \in \mathcal{D}} -\log f[x_i](y_i)q(\mathcal{E} = e_k | x_i, y_i) \right|. \quad (108)$$

Let \mathcal{D} and \mathcal{D}' be two identical datasets except for one data point $x_j \neq x'_j$. We have:

$$\Phi(\mathcal{D}) - \Phi(\mathcal{D}') \quad (109)$$

$$\leq \sup_{f \in \mathcal{V}, q \in \mathcal{Q}} \left[\left| q(\mathcal{E} = e_k)\mathbb{E}_q[-\log f[x](y)|\mathcal{E} = e_k] - \frac{1}{|\mathcal{D}|} \sum_{x_i, y_i \in \mathcal{D}} -\log f[x_i](y_i)q(\mathcal{E} = e_k | x_i, y_i) \right| \right] \quad (110)$$

$$- \left| q(\mathcal{E} = e_k)\mathbb{E}_q[-\log f[x](y)|\mathcal{E} = e_k] - \frac{1}{|\mathcal{D}'|} \sum_{x'_i, y'_i \in \mathcal{D}'} -\log f[x'_i](y'_i)q(\mathcal{E} = e_k | x'_i, y'_i) \right| \quad (111)$$

$$\leq \sup_{f \in \mathcal{V}, q \in \mathcal{Q}} \left| \frac{1}{|\mathcal{D}|} \sum_{x_i, y_i \in \mathcal{D}} -\log f[x_i](y_i)q(\mathcal{E} = e_k | x_i, y_i) - \frac{1}{|\mathcal{D}'|} \sum_{x'_i, y'_i \in \mathcal{D}'} -\log f[x'_i](y'_i)q(\mathcal{E} = e_k | x'_i, y'_i) \right| \quad (112)$$

$$= \sup_{f \in \mathcal{V}, q \in \mathcal{Q}} \frac{1}{|\mathcal{D}|} \left| \log f[x_j](y_j)q(\mathcal{E} = e_k | x_j, y_j) - \log f[x'_j](y'_j)q(\mathcal{E} = e_k | x'_j, y'_j) \right| \quad (113)$$

$$\leq \frac{2B}{|\mathcal{D}|}. \quad (114)$$

According to McDiarmid's inequality, for any $\delta \in (0, 1)$, with a probability over $1 - \delta$, we have:

$$\Phi(\mathcal{D}) \leq \mathbb{E}_{\mathcal{D}}[\Phi(\mathcal{D})] + B\sqrt{\frac{2\log\frac{1}{\delta}}{|\mathcal{D}|}}. \quad (115)$$

Next we derive a bound for $\mathbb{E}_{\mathcal{D}}[\Phi(\mathcal{D})]$. Consider a dataset \mathcal{D}' independently and identically drawn from $q(X, Y) = P(X, Y)$ with the same size as \mathcal{D} . We notice that

$$q(\mathcal{E} = e_k)\mathbb{E}_q[-\log f[x](y)|\mathcal{E} = e_k] = \mathbb{E}_{\mathcal{D}'}\left[-\frac{1}{|\mathcal{D}'|}\sum_{x'_i, y'_i \in \mathcal{D}'} -\log f[x'_i](y'_i)q(\mathcal{E} = e_k|x'_i, y'_i)\right]. \quad (116)$$

Thus, $\mathbb{E}_{\mathcal{D}}[\Phi(\mathcal{D})]$ could be reformulated as:

$$\mathbb{E}_{\mathcal{D}}[\Phi(\mathcal{D})] = \mathbb{E}_{\mathcal{D}}\left[\sup_{f \in \mathcal{V}, q \in \mathcal{Q}} \left| \mathbb{E}_{\mathcal{D}'}\left[-\frac{1}{|\mathcal{D}'|}\sum_{x'_i, y'_i \in \mathcal{D}'} -\log f[x'_i](y'_i)q(\mathcal{E} = e_k|x'_i, y'_i)\right] \right. \right. \quad (117)$$

$$\left. \left. -\frac{1}{|\mathcal{D}|}\sum_{x_i, y_i \in \mathcal{D}} -\log f[x_i](y_i)q(\mathcal{E} = e_k|x_i, y_i)\right| \right] \quad (118)$$

$$\leq \mathbb{E}_{\mathcal{D}}\left[\sup_{f \in \mathcal{V}, q \in \mathcal{Q}} \mathbb{E}_{\mathcal{D}'}\left[-\frac{1}{|\mathcal{D}'|}\sum_{x'_i, y'_i \in \mathcal{D}'} -\log f[x'_i](y'_i)q(\mathcal{E} = e_k|x'_i, y'_i)\right. \right. \quad (119)$$

$$\left. \left. -\frac{1}{|\mathcal{D}|}\sum_{x_i, y_i \in \mathcal{D}} -\log f[x_i](y_i)q(\mathcal{E} = e_k|x_i, y_i)\right| \right] \quad (120)$$

$$\leq \mathbb{E}_{\mathcal{D}, \mathcal{D}'}\left[\sup_{f \in \mathcal{V}, q \in \mathcal{Q}} \frac{1}{|\mathcal{D}|}\left|\sum_{x_i, y_i \in \mathcal{D}} \log f[x_i](y_i)q(\mathcal{E} = e_k|x_i, y_i)\right. \right. \quad (121)$$

$$\left. \left. -\sum_{x'_i, y'_i \in \mathcal{D}'} \log f[x'_i](y'_i)q(\mathcal{E} = e_k|x'_i, y'_i)\right| \right] \quad (122)$$

$$\left. \left. -\sum_{x'_i, y'_i \in \mathcal{D}'} \sigma_i \log f[x'_i](y'_i)q(\mathcal{E} = e_k|x'_i, y'_i)\right| \right] \quad (123)$$

$$\leq \mathbb{E}_{\mathcal{D}, \sigma}\left[\sup_{f \in \mathcal{V}, q \in \mathcal{Q}} \frac{1}{|\mathcal{D}|}\left|\sum_{x_i, y_i \in \mathcal{D}} \sigma_i \log f[x_i](y_i)q(\mathcal{E} = e_k|x_i, y_i)\right| \right] \quad (124)$$

$$+ \mathbb{E}_{\mathcal{D}', \sigma}\left[\sup_{f \in \mathcal{V}, q \in \mathcal{Q}} \frac{1}{|\mathcal{D}'|}\left|\sum_{x'_i, y'_i \in \mathcal{D}'} \sigma_i \log f[x'_i](y'_i)q(\mathcal{E} = e_k|x'_i, y'_i)\right| \right] \quad (125)$$

$$= 2\mathcal{R}_{|\mathcal{D}|}(\mathcal{G}_{\mathcal{V}}^k), \quad (126)$$

where σ_i are independent Rademacher variables. Equation 121 follows from Jensen's inequality and the convexity of sup. Equation 123 holds due to the symmetry of $\log f[x_i](y_i)q(\mathcal{E} = e_k|x_i, y_i) - \log f[x'_i](y'_i)q(\mathcal{E} = e_k|x'_i, y'_i)$ and the argument that Rademacher variables preserve the expected sum of symmetric random variables with a convex mapping (Ledoux and Talagrand (1991), Lemma 6.3).

Substituting Equation 126 to Equation 115, we have for any $\delta \in (0, 1)$, with a probability over $1 - \delta$, $\forall f \in \mathcal{V}$, $\forall q \in \mathcal{Q}$, the following holds:

$$\left| q(\mathcal{E} = e_k) \mathbb{E}_q [-\log f[x](y) | \mathcal{E} = e_k] - \frac{1}{|\mathcal{D}|} \sum_{x_i, y_i \in \mathcal{D}} -\log f[x_i](y_i) q(\mathcal{E} = e_k | x_i, y_i) \right| \quad (127)$$

$$\leq 2\mathcal{R}_{|\mathcal{D}|}(\mathcal{G}_{\mathcal{V}}^k) + B \sqrt{\frac{2 \log \frac{1}{\delta}}{|\mathcal{D}|}}. \quad (128)$$

Let $\tilde{f}_k = \arg \inf_f \{q(\mathcal{E} = e_k) \mathbb{E}_q [-\log f[x](y) | \mathcal{E} = e_k]\}$.

Let $\hat{f}_k = \arg \inf_f \{\frac{1}{|\mathcal{D}|} \sum_{x_i, y_i \in \mathcal{D}} -\log f[x_i](y_i) q(\mathcal{E} = e_k | x_i, y_i)\}$.

Now we have

$$q(\mathcal{E} = e_k) \mathbb{E}_q [-\log \tilde{f}_k[x](y) | \mathcal{E} = e_k] - \frac{1}{|\mathcal{D}|} \sum_{x_i, y_i \in \mathcal{D}} -\log \tilde{f}_k[x_i](y_i) q(\mathcal{E} = e_k | x_i, y_i) \quad (129)$$

$$\leq q(\mathcal{E} = e_k) H_{\mathcal{V}}(Y | X, \mathcal{E} = e_k) - \frac{1}{|\mathcal{D}|} \sum_{x_i, y_i \in \mathcal{D}} -\log \hat{f}_k[x_i](y_i) q(\mathcal{E} = e_k | x_i, y_i) \quad (130)$$

$$\leq q(\mathcal{E} = e_k) \mathbb{E}_q [-\log \hat{f}_k[x](y) | \mathcal{E} = e_k] - \frac{1}{|\mathcal{D}|} \sum_{x_i, y_i \in \mathcal{D}} -\log \hat{f}_k[x_i](y_i) q(\mathcal{E} = e_k | x_i, y_i). \quad (131)$$

Combining Equation 127 and Equation 129-131, the lemma is proved. \blacksquare

Lemma 15 Assume $\forall x \in \mathcal{X}, \forall y \in \mathcal{Y}, \forall f \in \mathcal{V}$, $\log f[\emptyset](y) \in [-B, B]$ where $B > 0$. The definition of $\mathcal{G}_{\mathcal{V}}^k$ and $\mathcal{R}_N(\mathcal{G})$ follows from Lemma 14. Define $\hat{f}_k = \arg \inf_f \{\frac{1}{|\mathcal{D}|} \sum_{x_i, y_i \in \mathcal{D}} -\log f[\emptyset](y_i) q(\mathcal{E} = e_k | x_i, y_i)\}$.

Then for any $q \in \mathcal{Q}$, any $\delta \in (0, 1)$, with a probability over $1 - \delta$, we have

$$\left| q(\mathcal{E} = e_k) H_{\mathcal{V}}(Y | \mathcal{E} = e_k) - \frac{1}{|\mathcal{D}|} \sum_{x_i, y_i \in \mathcal{D}} -\log \hat{f}_k[\emptyset](y_i) q(\mathcal{E} = e_k | x_i, y_i) \right| \quad (132)$$

$$\leq 2\mathcal{R}_{|\mathcal{D}|}(\mathcal{G}_{\mathcal{V}}^k) + B \sqrt{\frac{2 \log \frac{1}{\delta}}{|\mathcal{D}|}}. \quad (133)$$

Proof Similar to Lemma 14, we could prove that

$$\left| q(\mathcal{E} = e_k) H_{\mathcal{V}}(Y | \mathcal{E} = e_k) - \frac{1}{|\mathcal{D}|} \sum_{x_i, y_i \in \mathcal{D}} -\log \hat{f}_k[\emptyset](y_i) q(\mathcal{E} = e_k | x_i, y_i) \right| \quad (134)$$

$$\leq 2\mathcal{R}_{|\mathcal{D}|}(\mathcal{G}_{\mathcal{V}^{\emptyset}}^k) + B \sqrt{\frac{2 \log \frac{1}{\delta}}{|\mathcal{D}|}}, \quad (135)$$

where $\mathcal{G}_{\mathcal{V}^{\emptyset}}^k = \{g | g(x, y) = \log f[\emptyset](y) q(\mathcal{E} = e_k | x, y), f \in \mathcal{V}, q \in \mathcal{Q}\}$.

According to the definition for the predictive family \mathcal{V} (Xu et al. (2020), Definition 1), $\forall f \in \mathcal{V}$, there exists $f' \in \mathcal{V}$ such that $\forall x \in \mathcal{X}$, $f[\emptyset] = f'[x]$. Thus, $\mathcal{G}_{\mathcal{V}^k}^k \subset \mathcal{G}_{\mathcal{V}^k}$, and therefore $\mathcal{R}_{|\mathcal{D}|}(\mathcal{G}_{\mathcal{V}^k}^k) \leq \mathcal{R}_{|\mathcal{D}|}(\mathcal{G}_{\mathcal{V}^k}^k)$. Substituting into Equation 134, the lemma is proved. \blacksquare

Lemma 16 ((Xu et al., 2020), Theorem 1) *Assume $\forall x \in \mathcal{X}, \forall y \in \mathcal{Y}, \forall f \in \mathcal{V}$, $\log f[x](y) \in [-B, B]$ where $B > 0$. Define a function class $\mathcal{G}_{\mathcal{V}}^* = \{g | g(x, y) = \log f[x](y), f \in \mathcal{V}\}$. The definition of $\mathcal{R}_N(\mathcal{G})$ follows from Lemma 14.*

Then for any $\delta \in (0, 0.5)$, with a probability over $1 - 2\delta$, we have

$$\left| \mathbb{I}_{\mathcal{V}}(X \rightarrow Y) - \hat{\mathbb{I}}_{\mathcal{V}}(X \rightarrow Y) \right| \leq 4\mathcal{R}_{|\mathcal{D}|}(\mathcal{G}_{\mathcal{V}}^*) + 2B\sqrt{\frac{2\log \frac{1}{\delta}}{|\mathcal{D}|}}. \quad (136)$$

Finally we are prepared to prove Theorem 11.

Proof [Proof of Theorem 11] We first bound the error of empirical estimation with the sum of items in Lemma 14,15,16.

$$|\mathcal{H}_{\mathcal{V}}^{\mathcal{E}_K}(X \rightarrow Y) - \hat{H}_{\mathcal{V}}^{\mathcal{E}_K}(X \rightarrow Y; \mathcal{D})| \quad (137)$$

$$\leq \left| \sup_{\mathcal{E} \in \mathcal{E}_K} \mathbb{I}_{\mathcal{V}}(X \rightarrow Y | \mathcal{E}) - \sup_{\mathcal{E} \in \mathcal{E}_K} \hat{\mathbb{I}}_{\mathcal{V}}(X \rightarrow Y | \mathcal{E}; \mathcal{D}) \right| + \left| \mathbb{I}_{\mathcal{V}}(X \rightarrow Y) - \hat{\mathbb{I}}_{\mathcal{V}}(X \rightarrow Y; \mathcal{D}) \right| \quad (138)$$

$$\leq \sup_{\mathcal{E} \in \mathcal{E}_K} \left| \mathbb{I}_{\mathcal{V}}(X \rightarrow Y | \mathcal{E}) - \hat{\mathbb{I}}_{\mathcal{V}}(X \rightarrow Y | \mathcal{E}; \mathcal{D}) \right| + \left| \mathbb{I}_{\mathcal{V}}(X \rightarrow Y) - \hat{\mathbb{I}}_{\mathcal{V}}(X \rightarrow Y; \mathcal{D}) \right| \quad (139)$$

$$= \sup_{q \in \mathcal{Q}} \left| \sum_{k=1}^K [q(\mathcal{E} = e_k) H_{\mathcal{V}}(Y | \mathcal{E} = e_k) - q(\mathcal{E} = e_k) H_{\mathcal{V}}(Y | X, \mathcal{E} = e_k)] \right. \quad (140)$$

$$\left. - \sum_{k=1}^K [q(\mathcal{E} = e_k) \hat{H}_{\mathcal{V}}(Y | \mathcal{E} = e_k; \mathcal{D}) - q(\mathcal{E} = e_k) \hat{H}_{\mathcal{V}}(Y | X, \mathcal{E} = e_k; \mathcal{D})] \right| \quad (141)$$

$$+ \left| \mathbb{I}_{\mathcal{V}}(X \rightarrow Y) - \hat{\mathbb{I}}_{\mathcal{V}}(X \rightarrow Y; \mathcal{D}) \right| \quad (142)$$

$$\leq \sum_{k=1}^K \sup_{q \in \mathcal{Q}} \left| q(\mathcal{E} = e_k) H_{\mathcal{V}}(Y | \mathcal{E} = e_k) - q(\mathcal{E} = e_k) \hat{H}_{\mathcal{V}}(Y | \mathcal{E} = e_k; \mathcal{D}) \right| \quad (143)$$

$$+ \sum_{k=1}^K \sup_{q \in \mathcal{Q}} \left| q(\mathcal{E} = e_k) H_{\mathcal{V}}(Y | X, \mathcal{E} = e_k) - q(\mathcal{E} = e_k) \hat{H}_{\mathcal{V}}(Y | X, \mathcal{E} = e_k; \mathcal{D}) \right| \quad (144)$$

$$+ \left| \mathbb{I}_{\mathcal{V}}(X \rightarrow Y) - \hat{\mathbb{I}}_{\mathcal{V}}(X \rightarrow Y; \mathcal{D}) \right| \quad (145)$$

$$= \sum_{k=1}^K \sup_{q \in \mathcal{Q}} \left| q(\mathcal{E} = e_k) H_{\mathcal{V}}(Y | \mathcal{E} = e_k) - \frac{1}{|\mathcal{D}|} \sum_{x_i, y_i \in \mathcal{D}} -\log \hat{f}_k[x_i](y_i) q(\mathcal{E} = e_k | x_i, y_i) \right| \quad (146)$$

$$+ \sum_{k=1}^K \sup_{q \in \mathcal{Q}} \left| q(\mathcal{E} = e_k) H_{\mathcal{V}}(Y | X, \mathcal{E} = e_k) - \frac{1}{|\mathcal{D}|} \sum_{x_i, y_i \in \mathcal{D}} -\log \hat{f}'_k[\emptyset](y_i) q(\mathcal{E} = e_k | x_i, y_i) \right| \quad (147)$$

$$+ \left| \mathbb{I}_{\mathcal{V}}(X \rightarrow Y) - \hat{\mathbb{I}}_{\mathcal{V}}(X \rightarrow Y; \mathcal{D}) \right|, \quad (148)$$

where $\hat{f}_k = \arg \inf_f \frac{1}{|\mathcal{D}|} \sum_{x_i, y_i \in \mathcal{D}} -\log f[x_i](y_i) q(\mathcal{E} = e_k | x_i, y_i)$,

and $\hat{f}'_k = \arg \inf_f \frac{1}{|\mathcal{D}|} \sum_{x_i, y_i \in \mathcal{D}} -\log f[\emptyset](y_i)q(\mathcal{E} = e_k|x_i, y_i)$, for any $q \in \mathcal{Q}$ and $1 \leq k \leq K$.

For simplicity, let

$$\text{Err}_k = \sup_{q \in \mathcal{Q}} \left| q(\mathcal{E} = e_k)H_{\mathcal{V}}(Y|X, \mathcal{E} = e_k) - \frac{1}{|\mathcal{D}|} \sum_{x_i, y_i \in \mathcal{D}} -\log \hat{f}_k[x_i](y_i)q(\mathcal{E} = e_k|x_i, y_i) \right|. \quad (149)$$

$$\text{Err}'_k = \sup_{q \in \mathcal{Q}} \left| q(\mathcal{E} = e_k)H_{\mathcal{V}}(Y|X, \mathcal{E} = e_k) - \frac{1}{|\mathcal{D}|} \sum_{x_i, y_i \in \mathcal{D}} -\log \hat{f}'_k[\emptyset](y_i)q(\mathcal{E} = e_k|x_i, y_i) \right|. \quad (150)$$

$$\text{Err}^* = \left| \mathbb{I}_{\mathcal{V}}(X \rightarrow Y) - \hat{\mathbb{I}}_{\mathcal{V}}(X \rightarrow Y; \mathcal{D}) \right|. \quad (151)$$

Then, by Lemma 14,15,16,

$$\Pr \left[|\mathcal{H}_K^{\mathcal{V}} - \hat{\mathcal{H}}_K^{\mathcal{V}}(\mathcal{D})| > 4(K+1)\mathcal{R}_{|\mathcal{D}|}(\mathcal{G}_{\mathcal{V}}) + 2(K+1)B\sqrt{\frac{2\log \frac{1}{\delta}}{|\mathcal{D}|}} \right] \quad (152)$$

$$\leq \Pr \left[\sum_{i=1}^K \text{Err}_k + \sum_{i=1}^K \text{Err}'_k + \text{Err}^* > 4(K+1)\mathcal{R}_{|\mathcal{D}|}(\mathcal{G}_{\mathcal{V}}) + 2(K+1)B\sqrt{\frac{2\log \frac{1}{\delta}}{|\mathcal{D}|}} \right] \quad (153)$$

$$\leq \Pr \left[\sum_{i=1}^K \text{Err}_k + \sum_{i=1}^K \text{Err}'_k + \text{Err}^* > \sum_{k=1}^K 4\mathcal{R}_{|\mathcal{D}|}(\mathcal{G}_{\mathcal{V}}^k) + 4\mathcal{R}_{|\mathcal{D}|}(\mathcal{G}_{\mathcal{V}}^*) + 2(K+1)B\sqrt{\frac{2\log \frac{1}{\delta}}{|\mathcal{D}|}} \right] \quad (154)$$

$$+ \left(\text{Err}^* > 4\mathcal{R}_{|\mathcal{D}|}(\mathcal{G}_{\mathcal{V}}^*) + 2B\sqrt{\frac{2\log \frac{1}{\delta}}{|\mathcal{D}|}} \right) \quad (155)$$

$$+ \Pr \left[\text{Err}^* > 4\mathcal{R}_{|\mathcal{D}|}(\mathcal{G}_{\mathcal{V}}^*) + 2B\sqrt{\frac{2\log \frac{1}{\delta}}{|\mathcal{D}|}} \right] \quad (156)$$

$$\leq 2(K+1)\delta. \quad (157)$$

Equation 154 is because of $\mathcal{G}_{\mathcal{V}}^k = \mathcal{G}_{\mathcal{V}}$, $\mathcal{G}_{\mathcal{V}}^* \subset \mathcal{G}_{\mathcal{V}}$ and therefore $R_{|\mathcal{D}|}(\mathcal{G}_{\mathcal{V}}^k) \leq R_{|\mathcal{D}|}(\mathcal{G}_{\mathcal{V}})$, $R_{|\mathcal{D}|}(\mathcal{G}_{\mathcal{V}}^*) \leq R_{|\mathcal{D}|}(\mathcal{G}_{\mathcal{V}})$. Hence,

$$\Pr \left[|\mathcal{H}_{\mathcal{V}}^{\mathcal{E}_K}(X \rightarrow Y) - \hat{H}_{\mathcal{V}}^{\mathcal{E}_K}(X \rightarrow Y; \mathcal{D})| \leq 4(K+1)\mathcal{R}_{|\mathcal{D}|}(\mathcal{G}_{\mathcal{V}}) + 2(K+1)B\sqrt{\frac{2\log \frac{1}{\delta}}{|\mathcal{D}|}} \right] \quad (158)$$

$$\geq 1 - 2(K+1)\delta. \quad (159)$$

■

Appendix E. Proof of Theorem 12

Proof [Proof of Theorem 12] The objective function of our IM algorithm is directly derived from the definition of empirical predictive heterogeneity in Definition 10. For the regression task, we assume the predictive family as

$$\mathcal{V}_1 = \{g : g[x] = \mathcal{N}(f_{\theta}(x), \sigma^2), f \text{ is the regression model and } \theta \text{ is learnable, } \sigma = 1.0(\text{fixed})\}, \quad (160)$$

where we only care about the output of the model and the noise scale of the Gaussian distribution is often ignored, for which we simply set $\sigma = 1.0$ as a fixed term. Then for each environment $e \in \text{supp}(\mathcal{E}^*)$, the $\mathbb{I}_V(X \rightarrow Y|\mathcal{E}^* = e)$ becomes

$$\mathbb{I}_V(X \rightarrow Y|\mathcal{E}^* = e) \propto \min_{\theta} \mathbb{E}[\|Y - f_{\theta}(X)\|^2|\mathcal{E}^* = e] - \text{Var}(Y|\mathcal{E}^*), \quad (161)$$

which corresponds with the MSE loss and the proposed regularizer in Equation 35. For the classification task, the derivation is similar, and the regularizer becomes the entropy of Y in sub-population e and the loss function becomes the cross-entropy loss. ■

References

- Martin Arjovsky, Léon Bottou, Ishaan Gulrajani, and David Lopez-Paz. Invariant risk minimization. *arXiv preprint arXiv:1907.02893*, 2019.
- Peter L Bartlett and Shahar Mendelson. Rademacher and gaussian complexities: Risk bounds and structural results. *JMLR*, 3(Nov):463–482, 2002.
- SM Chan, LD Ying, JM Morton, and S Ghiassi. Gastrointestinal manifestations of covid-19 mimicking a surgical abdomen. *American College of Surgeons*, 2022.
- M Cover Thomas and A Thomas Joy. Elements of information theory. *New York: Wiley*, 3:37–38, 1991.
- Elliot Creager, Jörn-Henrik Jacobsen, and Richard Zemel. Environment inference for invariant learning. In *ICML*, pages 2189–2200. PMLR, 2021.
- Peng Cui and Susan Athey. Stable learning establishes some common ground between causal inference and machine learning. *Nature Machine Intelligence*, 4(2):110–115, 2022.
- John Duchi, Tatsunori Hashimoto, and Hongseok Namkoong. Distributionally robust losses for latent covariate mixtures. *Operations Research*, 2022.
- Jianqing Fan, Fang Han, and Han Liu. Challenges of big data analysis. *National science review*, 1(2):293–314, 2014.
- Subash Ghimire, Sachit Sharma, Achint Patel, Rasmita Budhathoki, Raja Chakinala, Hafiz Khan, Matthew Lincoln, and Michael Georgeston. Diarrhea is associated with increased severity of disease in covid-19: Systemic review and metaanalysis. *SN Comprehensive Clinical Medicine*, pages 1–8, 2021.
- Moritz Hardt, Eric Price, and Nati Srebro. Equality of opportunity in supervised learning. *Advances in neural information processing systems*, 29, 2016.
- James J Heckman. Sample selection bias as a specification error. *Econometrica: Journal of the econometric society*, pages 153–161, 1979.
- Sunyea Helal. Subgroup discovery algorithms: a survey and empirical evaluation. *Journal of computer science and technology*, 31(3):561–576, 2016.

- Miguel A Hernán, David Clayton, and Niels Keiding. The simpson’s paradox unraveled. *International journal of epidemiology*, 40(3):780–785, 2011.
- R. Kohavi and B. Becker. *Adult*, 1996.
- Masanori Koyama and Shoichiro Yamaguchi. Out-of-distribution generalization with maximal invariant predictor. 2020.
- Michel Ledoux and Michel Talagrand. *Probability in Banach Spaces: isoperimetry and processes*, volume 23. Springer Science & Business Media, 1991.
- H Li and JF Reynolds. On definition and quantification of heterogeneity. *Oikos*, pages 280–284, 1995.
- Jiashuo Liu, Zheyuan Hu, Peng Cui, Bo Li, and Zheyuan Shen. Heterogeneous risk minimization. In *ICML*, pages 6804–6814. PMLR, 2021a.
- Jiashuo Liu, Zheyuan Shen, Peng Cui, Linjun Zhou, Kun Kuang, and Bo Li. Distributionally robust learning with stable adversarial training. *IEEE Transactions on Knowledge and Data Engineering*, 2022.
- Jue Liu, Liyuan Tao, Xia Liu, Hongyan Yao, Shicheng Yu, Qiqi Wang, Jiaojiao Zhang, Zhancheng Gao, Rongmeng Jiang, Wenzhan Jing, and Min Liu. Gi symptoms and fever increase the risk of severe illness and death in patients with covid-19. *Gut*, 70(2):442–444, 2021b. ISSN 0017-5749. doi: 10.1136/gutjnl-2020-321751. URL <https://gut.bmj.com/content/70/2/442>.
- David B Lobell, Marshall B Burke, Claudia Tebaldi, Michael D Mastrandrea, Walter P Falcon, and Rosamond L Naylor. Prioritizing climate change adaptation needs for food security in 2030. *Science*, 319(5863):607–610, 2008.
- Todd K Moon. The expectation-maximization algorithm. *IEEE Signal processing magazine*, 13(6):47–60, 1996.
- Jonas Peters, Peter Bühlmann, and Nicolai Meinshausen. Causal inference by using invariant prediction: identification and confidence intervals. *Journal of the Royal Statistical Society: Series B (Statistical Methodology)*, 78(5):947–1012, 2016.
- Douglas A Reynolds. Gaussian mixture models. *Encyclopedia of biometrics*, 741(659-663), 2009.
- Michael Roberts, Derek Driggs, Matthew Thorpe, Julian Gilbey, Michael Yeung, Stephan Ursprung, Angelica I Aviles-Rivero, Christian Etmann, Cathal McCague, Lucian Beer, et al. Common pitfalls and recommendations for using machine learning to detect and prognosticate for covid-19 using chest radiographs and ct scans. *Nature Machine Intelligence*, 3(3):199–217, 2021.
- Paul R Rosenbaum. Heterogeneity and causality: Unit heterogeneity and design sensitivity in observational studies. *The American Statistician*, 59(2):147–152, 2005.

- Shiori Sagawa, Pang Wei Koh, Tatsunori B Hashimoto, and Percy Liang. Distributionally robust neural networks for group shifts: On the importance of regularization for worst-case generalization. *arXiv preprint arXiv:1911.08731*, 2019.
- Amirreza Shaban, Ching-An Cheng, Nathan Hatch, and Byron Boots. Truncated back-propagation for bilevel optimization. In *The 22nd International Conference on Artificial Intelligence and Statistics*, pages 1723–1732. PMLR, 2019.
- Zheyuan Shen, Jiashuo Liu, Yue He, Xingxuan Zhang, Renzhe Xu, Han Yu, and Peng Cui. Towards out-of-distribution generalization: A survey. 2021.
- E. Tipton, J. Spybrook, K. G. Fitzgerald, Q. Wang, and C. Davidson. Toward a system of evidence for all: Current practices and future opportunities in 37 randomized trials. *Educational Researcher*, page 0013189X2096068, 2020.
- Shikha Verma. Weapons of math destruction: how big data increases inequality and threatens democracy. *Vikalpa*, 44(2):97–98, 2019.
- Clifford H Wagner. Simpson’s paradox in real life. *The American Statistician*, 36(1):46–48, 1982.
- Xiao Wang, Houye Ji, Chuan Shi, Bai Wang, Yanfang Ye, Peng Cui, and Philip S Yu. Heterogeneous graph attention network. In *WWW*, pages 2022–2032, 2019.
- Christopher Winship and Robert D Mare. Models for sample selection bias. *Annual review of sociology*, pages 327–350, 1992.
- Laure Wynants, Ben Van Calster, Gary S Collins, Richard D Riley, Georg Heinze, Ewoud Schuit, Marc MJ Bonten, Darren L Dahly, Johanna A Damen, Thomas PA Debray, et al. Prediction models for diagnosis and prognosis of covid-19: systematic review and critical appraisal. *bmj*, 369, 2020.
- Yilun Xu, Shengjia Zhao, Jiaming Song, Russell Stewart, and Stefano Ermon. A theory of usable information under computational constraints. In *ICLR*, 2020.
- W. Zeng, K. Qi, M. Ye, L. Zheng, and Y. Wei. Gastrointestinal symptoms are associated with severity of coronavirus disease 2019: a systematic review and meta-analysis. *European Journal of Gastroenterology & Hepatology*, Publish Ahead of Print, 2021.
- Shengjia Zhao, Abhishek Sinha, Yutong He, Aidan Perreault, Jiaming Song, and Stefano Ermon. Comparing distributions by measuring differences that affect decision making. In *International Conference on Learning Representations*, 2021.
- Peijie Zhong, Jing Xu, Dong Yang, Yue Shen, and Yangbai Sun. Covid-19-associated gastrointestinal and liver injury: clinical features and potential mechanisms. *Signal Transduction and Targeted Therapy*, 5(1):256, 2020.
- Xiao Zhou, Yong Lin, Renjie Pi, Weizhong Zhang, Renzhe Xu, Peng Cui, and Tong Zhang. Model agnostic sample reweighting for out-of-distribution learning. In *International Conference on Machine Learning*, pages 27203–27221. PMLR, 2022.